Technische Universität München
TUM School of Medicine and Health

Cannula Insertion in Big-Bubble Deep Anterior Lamellar Keratoplasty: Comparison of Robot-assisted and Manual Performance in a Porcine Eye Model Simulation

Anne-Marie Jablonka

Vollständiger Abdruck der von der TUM School of Medicine and Health der Technischen Universität München zur Erlangung einer

Doktorin der Medizin (Dr. med.)

genehmigten Dissertation.

Vorsitz: apl. Prof. Dr. Bernhard Haslinger

Prüfende der Dissertation:

1. Prof. Dr. Mathias M. Maier
2. Priv.-Doz. Dr.-Ing. Mohammad Ali Nasseri

Die Dissertation wurde am 30.10.2024 bei der Technischen Universität München eingereicht und durch die TUM School of Medicine and Health am 30.04.2025 angenommen.

TABLE OF CONTENTS

TABLE OF ILLUSTRATIONS

8. Illustration 8. **- 40 –**

An example of successful deep air injection.

9. Illustration 9. **- 45 -**

Examples of OCT-acquisitions of cannula entry angle relative to the cornea’s central surface.

TABLE OF TABLES

ABBREVIATIONS

ALK	Anterior Lamellar Keratoplasty
BL	Bowman's Layer
DALK	Deep Anterior Lamellar Keratoplasty
DM	Descemet Membrane
DMEK	Descemet Membrane Endothelial Keratoplasty
DSAEK	Descemet Stripping Automated Endothelial Keratoplasty
DSEK	Descemet Stripping Endothelial Keratoplasty
LK	Lamellar Keratoplasty
OCT	Optical Coherence Tomography
PDL	Pre-Descemet Layer
PKP	Penetrating Keratoplasty
SALK	Superficial Anterior Lamellar Keratoplasty

0. SUMMARY

Among clinical surgical procedures, ophthalmic surgical interventions are considered the most challenging for numerous reasons. The eye is composed of delicate structures and is thus considered a difficult operational field. Surgical manipulation generally requires working with a microscope. The handling of the instruments, suturing and simultaneous monitoring demands high concentration, a good hand-eye-coordination and therefore, a lot of practice. Mistakes can potentially lead to blindness or loss of the eye.

Corneal transplantation may be considered one of the most important ophthalmic surgeries. The clear cornea acts as an anatomical barrier of the eye bulb whilst permitting light entrance and accounting for most of the eye's refractive power. Replacing damaged or opaque corneal tissue by a human transplant can potentially restore the eye's physical integrity as well as improve visual acuity.
However, transplantation techniques are challenging operations that require manipulation with a high degree of precision. Some procedures show high failure rates, albeit conducted by experienced individuals.

Big-Bubble DALK is a transplantation technique that is associated with a low probability of graft rejection and thus, long durability of the transplant, whilst showing similarly good outcomes in postoperative visual acuity as penetrating keratoplasty. However, in Big-Bubble DALK, particularly high failure rates are observed.
The procedure requires the insertion of an air-filled cannula into the corneal stroma to dissect the target corneal layers by air injection (i.e., Big-Bubble formation). A sufficient depth needs to be reached to successfully achieve dissection, whilst at the

same time avoiding perforation. As the cornea measures only 550 microns in thickness, this is a conceivably difficult task. Perforation is a frequently observed incidence.

This work aims to investigate potential facilitation of Big-Bubble DALK by implementing robotic assistance coupled with intraoperative imaging. For this purpose, cannula insertion and air injection following the Big-Bubble technique were simulated with and without robotic assistance, whilst monitored in real-time using intraoperative Optical Coherence Tomography.

The experimental simulations were conducted on porcine eyes by two novice surgeons with no prior experience in experimental or clinical ophthalmic surgery.

The results showed a significantly deeper cannula insertion into the corneal stroma in robot-assisted trials (mean 89 %) as compared to manual trials (mean 85%), without perforation respectively. Cannula insertion at a depth of at least 79% has been shown to be associated with successful pneumo-dissection of the corneal layers, which in turn is an essential prerequisite for successful DALK-transplantation.

1. INTRODUCTION

1.1 Anatomy of the human eye

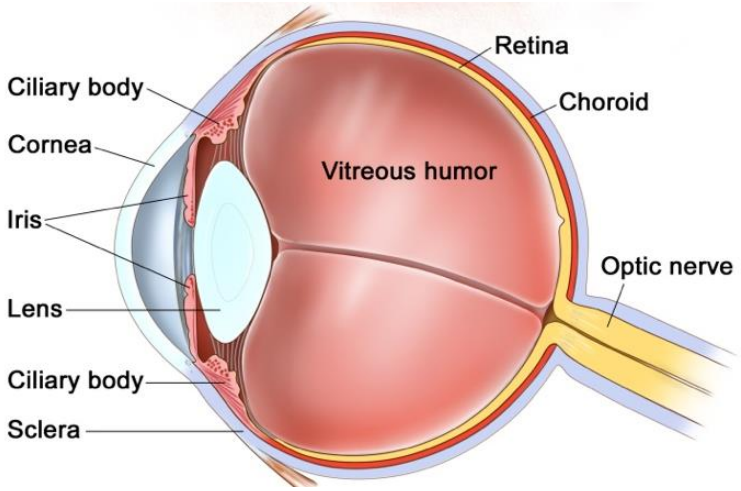

Illustration 1. **Anatomical structures of the human eye.** [image source: F1]

The eyeball, or bulbus oculi, lies inside the orbital cavity and is enveloped by extrinsic ocular muscles, the tenon's capsule and the protective fatty tissue of the orbit. The bulbus consists of a three-layered wall: the sclera, the uvea, and the retina. The retina is the innermost layer and acts as the sensory epithelium. Neurosensory information is conducted to the brain via the optic nerve (see *Illustration 1*).

The uvea, or pigmented epithelium, is separated into the choroid, iris, and ciliary body. The choroid or vascular layer carries blood vessels that are providing the organ with oxygen and nutrients; the iris regulates pupil size and thus the amount of light reaching the retina. The ciliary body has two main functions: It produces aqueous humor, a low protein blood filtrate that maintains the intraocular pressure and carries nutrients and immunoglobulins. Second, it connects to the crystalline lens' capsule via suspensory

ligaments. Contraction and relaxation of the ciliary muscle cause stretching or relaxing of the ligaments which transfer the force onto the lens. The change in the lens' shape effect a change of refraction and thus cause accommodation. The lens has a refractive power of approximately 18 diopters.

Lens, aqueous humor, and the cornea compose the refractive media.

The cornea is a transparent structure bordering with the sclera at the corneal limbus and comprising the anterior chamber of the eye along with the iris and the lens. The cornea's refractive power is approximately 43 diopters, which accounts for 2/3 of the eye's total refractive power (Patel & Tutchenko, 2019).

1.1.1 Anatomy of the cornea in detail: Composition and layers

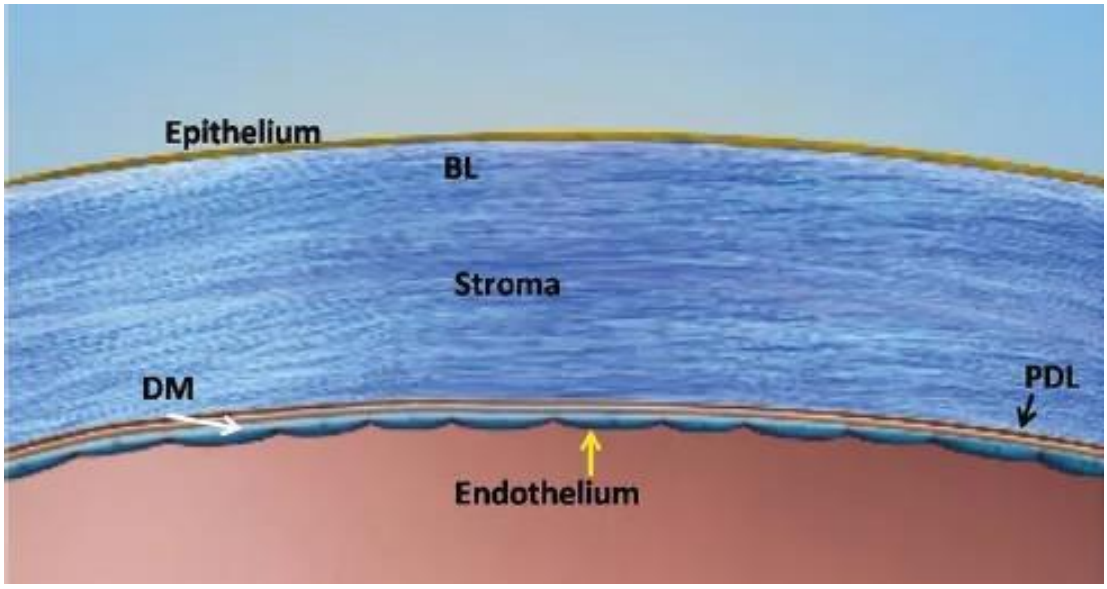

Illustration 2. **Corneal layers, including presumed location of Dua's Layer.**

BL: Bowman's Layer; PDL: Pre-Descemet-Layer, or Dua's Layer; DM: Descemet Membrane. Note: The presumed location of PDL, or Dua's Layer, is indicated. [Image source: F2]

The cornea on average measures about 11,5 mm in diameter and 120 mm^2 in surface. Its thickness measures 540-550 microns on average in its center and 600-800 microns at its periphery (Khaja et al., 2015). For the large part, it is composed of collagen type I fibers, whose compact arrangement enables transparency (Del,Monte & Kim, 2011).

The cornea does not carry any blood vessels but is densely innervated. It is one of the most sensitive tissues of the body. The sensory fibers are branches deriving from the ophthalmic stem (V1) of Nervus trigeminus.

It is largely agreed upon that the cornea can be histologically divided into five layers (Sridhar, 2018); however recent research suggests the existence of a possible sixth layer, namely Dua's Layer, presumably located between the corneal stroma and the Descemet's membrane.

The five corneal layers, as they are found in humans and other primates, are shown in *Illustration 2*. They include 1) Corneal epithelium, which is in contact with the surrounding atmosphere and consists of regeneratable cells, 2) Bowman's layer, which is acellular and consists mainly of type I collagen fibers, 3) Corneal stroma, making up 90% of the corneal thickness and consisting of type I collagen fibers, 4) Descemet's membrane (DM), an acellular layer mainly composed of type IV collagen, and 5) Endothelium, the innermost layer that is directly in contact with the aqueous humor. It is consisting of a monolayer of low-cuboidal cells that are actively regulating fluid transport between the cornea and the aqueous humor (DelMonte & Kim, 2011).

Dua's layer is presumed to be located just anterior to the DM, thus it is referred to as Pre-Descement-Layer (PDL) (Dua et al., 2013) (see *Illustration 2*).

For the scope of this work, PDL is not going to be specifically outlined, but shall be understood when referring to stroma or pre-Descemet corneal layers.

1.2 Corneal diseases

The healthy cornea has a regular aspheric curvature and follows a typical thickness profile (see 1.1.1). It is transparent and consequently vessel-free with all its layers intact.

Irregular corneal curvature, i.e., astigmatism, increase or decrease in thickness, opacities, or damage in one or more corneal layers affect entrance of light and refraction of light and consequently, vision. It is important to note that certain refractive irregularities can be aided by visual aids such as glasses or contact lenses, however these measures may not be sufficient. Underlying tissue damage can furthermore promote infection, as there may be no sufficient barrier for pathogenic microorganisms (Al-Mujaini et al., 2009). Eye pain or irritation are further common symptoms.

The integrity of the cornea is based on numerous factors. For instance, a vital corneal epithelium is largely dependent on a healthy tear film, which contains immunocompetent substances and additionally functions as mechanical protection. An even distribution of tear film can in turn only be insured by proper lid function and so on (Dartt & Willcox, 2013).

Followingly, corneal diseases will be categorized by underlying cause, namely trauma, inflammation, degeneration, and dystrophy. Many corneal disorders however, such as Keratoconus, most likely underly multifactorial genesis (Gajecka & Nowak, 2011).

1.2.1 Trauma

Contact with harmful substances such as corrosive chemicals or penetration by a foreign body may cause corneal lesions throughout the corneal layers up to perforation.

Following trauma, the corneal layers can oftentimes reconstitute to a certain degree. In this context, scarring can occur, potentially leading to clouding or astigmatism and thus causing blurry vision or photosensitivity (Jain & Pineda, 2002; Barrientez et al., 2019).

1.2.2 Inflammation

Inflammation of the cornea, i.e., keratitis, can be caused by various factors, such as microbial infection (Al-Mujaini et al., 2009), (frequent) exposition to radiation (Izadi et al., 2018; Nuzzi et al., 2020), and exposition to harmful substances (Singh et al., 2013). Insufficient mechanical shielding or deficient immune reactions through abnormal tear film and/or lid function may cause or promote keratitis when other risk factors are present (Rosenberg & Eisen, 2008). Autoimmune reaction is known to be another frequent cause of keratitis and is oftentimes observed in patients with collagen vascular diseases such as rheumatoid arthritis (Cao et al., 2017).

Keratitis may result in corneal stippling, opacity, and epithelial or stromal edema. Post-inflammatory lesions can persist and cause scarring (Barr et al., 2006).

1.2.3 Degeneration

Corneal degeneration is a broad term for alterations of corneal tissue due to a multifactorial genesis. Degeneration may be involutional, i.e., age-related. For example, the elderly population may exhibit a basement membrane degeneration without an underlying disease, but due to involutional structural changes (Lorenzetti et al., 1967). Non-involutional degeneration may follow exposure to certain conditions such as inflammation or drugs. For example, calcific band keratopathy causes calcium salt to deposit in the Bowman's Membrane and anterior stroma. It more commonly affects patients with hypercalcemia, uveitis, or corneal inflammatory diseases. Deposits may be visually relevant by causing opacity or astigmatism (Merali, 2014). Depending on the type of degeneration, the corneal integrity can be harmed permanently (Stewart & Morrell, 2003).

1.2.4 Dystrophy

Corneal dystrophy, by definition, refers to a reduction in number or partial or total loss of function of cellular components of the cornea, following a genetic disorder or genetic disposition (Lin et al., 2016). Dystrophy can be limited to specific layers of the cornea, as it is the case in Fuchs Endothelial Dystrophy, which only affects the corneal endothelium (Adamis et al., 1993). Lattice dystrophy in turn is limited to the corneal stroma (Nakamura et al., 2000; Kivelä et al., 1993).

1.3 Corneal transplantation

1.3.1 Definition

Corneal transplantation, also referred to as corneal grafting, is a surgical procedure to replace diseased or damaged corneal tissue in a patient (i.e., host or recipient) by a donor's graft tissue. Graft corneas are typically organ donations obtained from deceased humans, which is referred to as allograft transplantation. Autograft transplantation in turn refers to grafting healthy corneal tissue of one individual's partner eye. It is a much less commonly performed procedure. Corneal grafts of animal origin are referred to as xenografts, whose potential implications are currently being researched (for instance, porcine corneal lenticules in treatment of Post-LASIK ectasia or Keratokonus (Fasolo et al., 2021; El-Massry et al., 2021).

Replacement of the affected cornea by material that will not work as active tissue is referred to as implantation (Krstic, 1985). For instance, the Boston keratoprosthesis is an artificial cornea made of synthetic material. It is commonly used in patients with severe corneal blindness (Nonpassopon et al., 2020).

1.3.2 Indications

Corneal transplantation is a therapeutic option when visually relevant corneal alterations cannot be treated conservatively by visual aids, medication, or surgical treatment other than transplantation, such as keratectomy (i.e., laser or manual excision of corneal tissue). This may be the case in corneas with a very high degree of astigmatism, oftentimes with extremely reduced thickness, or with scarring reaching in too great a depth for it to be completely removed by keratectomy (Pahor et al., 2007; Le et al., 2013).

Further typical indications for corneal transplantation include perforation of the cornea, corneal ulcers with associated danger of perforation, ubiquitous keratitis, and visually relevant opacity and scarring (Pahor et al., 2007; Le et al., 2017).

Patients with partially affected corneal layers can oftentimes be treated by transplantation of the affected layers only, which is referred to as lamellar transplantation (Espandar & Carlson, 2013; Ang et al., 2009). For instance, Fuchs endothelial dystrophy, affecting solely the corneal endothelium, can be treated by replacing the latter only. The utilized lamellar transplantation method is called Descemet Membrane Endothelial Keratoplasty, or DMEK (Ham et al., 2009). In turn, Keratokonus, in which DM and endothelium are typically intact, can be treated by lamellar transplantation of stroma anterior to the DM and endothelium. The procedure is called Deep Anterior Lamellar Keratoplasty, or DALK (Anwar & Teichmann, 2002). See 1.3.3 for detailed explanation of different corneal transplantation procedures.

1.3.3 Types of corneal transplantation

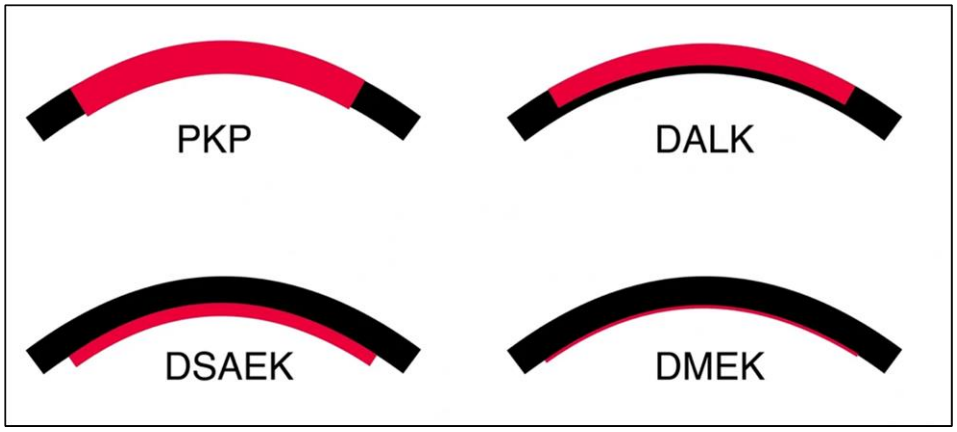

Illustration 3. **Types of corneal transplantation.**

PKP: Penetrating keratoplasty; DALK: Deep anterior lamellar keratoplasty; DSAEK: Descemet-stripping (automated) keratoplasty; DMEK: Descemet membrane endothelial keratoplasty. Corneal grafts are indicated in red. [Image source: F3]

1.3.3.1 Full-thickness or penetrating keratoplasty

As indicated by the name, in full-thickness penetrating keratoplasty (PKP) a full-thickness resection of the patient's cornea is performed and followingly replaced by a full-thickness corneal graft (see *Illustration 3*). The surgical procedure requires the penetration of all corneal layers (Moffatt et al., 2005). The graft is sutured to the host's cornea by interrupted or running sutures, which are typically removed after 12-24 months (Lee et al., 2012). Some corneal diseases, including inflammatory or infectious ulcerations or perforations, require immediate penetrating keratoplasty during an active inflammatory state (PKP à chaud) (Stübiger et al., 1995).

1.3.3.2 Partial-thickness or Lamellar keratoplasty: DMEK, DS(A)EK, ALK

As opposed to PKP, lamellar keratoplasty (LK) is used to replace corneal layers selectively (partial thickness keratoplasty).

Techniques that target deeper corneal layers include Descemet Membrane Endothelial Keratoplasty (DMEK), where DM and endothelium is replaced, and Descemet-stripping endothelial (automated) keratoplasty (DSEK/DS(A)EK), which additionally targets partial posterior stroma (Dapena et al., 2009). DSEK and DSAEK both target the same structures; however, the latter technique involves usage of an automated microkeratome for standardized donor graft preparation (Kocaba et al., 2018) (see *Illustration 3*).

Techniques that target superficial corneal layers are referred to as Anterior Lamellar Keratoplasty (ALK). ALK procedures include Superficial anterior Keratoplasty (SALK), which is limited to the removal and replacement of superficial stromal layers, and Deep Anterior Lamellar Keratoplasty (DALK), where all corneal layers anterior to the Descemet Membrane are being replaced (Espandar & Carlson, 2013) (see *Illustration 3*).

In 1.4, DALK will be described in greater detail, as a full understanding of the crucial surgical steps is essential to follow this work's purpose, the utilized experimental methods, and the results.

1.3.4 History of corneal transplantation

The idea of replacing opaque human corneas with clear protheses arose in the late 18th century. The utilization of animal donor corneas as replacement material has been suggested by Karl Himly in 1813, followed by initial experimental transplantation of animal corneas by Franz Riesinger in 1818. It was Riesinger who coined the term "keratoplasty". Later, the term "corneal transplantation" was introduced, followed by the first successful transplantation in a gazelle (Mannis & Krachmer, 1981).

In the following decades, the advancement of corneal transplantation was largely influenced by the experimental works conducted by Arthur von Hippel (1814 – 1916) and Henry Power (1829 – 1911) (McGhee et al., 2013).

Von Hippel invented the mechanical trephine, a device that facilitated excision of the donor and host cornea. Arguably, this made an invaluable contribution to improving excision techniques of corneal tissue (Mannis & Krachmer, 1981; McGhee et al., 2013). The device, in altered versions, is still in use today when performing penetrating and lamellar keratoplasty (Ng et al., 1995). Von Hippel conducted experimental and clinical transplantations in humans by trephining and removing the patient's anterior cornea and replacing the tissue with full-thickness xenografts. Therefore, the first transplantations to be attempted were technically lamellar keratoplasties.

The results showed varying degrees of success. However, in total, xenograft transplantation in humans remained rather unpromising.

In 1867, Power suggested usage of human allografts, which initiated a change of direction in experimental research. The first successful human allograft penetrating keratoplasty was conducted in 1905 by medical doctor Eduard Zirm (1877 – 1944). Since then, techniques for penetrating keratoplasty have undergone steady improvement and standardization, making it the gold standard for corneal transplantation up until the late 20th century (Moffatt et al., 2005).

1.3.4.1 Advancement of anterior lamellar keratoplasty

With penetrating keratoplasty being the dominant procedure in transplantation, research in lamellar transplantation techniques were pursued less intensely. However, attempts in lamellar techniques have regularly been reported. For instance, in 1908, Plange transplanted lamellar autografts, i.e., corneas obtained from a patient's partner eye

(Castillejo Becerra et al., 2023). These early attempts did not see much progress, as technically, the procedure remained challenging and generally resulted in poor visual outcomes, for example due to hazing of the interface.

However, severe postoperative complications were observed following penetrating keratoplasty, including for instance leakage of vitreous, secondary glaucoma, uveitis, and cataract. This led to re-pursuing research towards development of anterior lamellar keratoplasty techniques in the mid 20th-century, to ultimately improve long-term postoperative outcome (Ang et al., 2009; Tan & Anshu, 2009).

Hallermann, in 1959, was the first surgeon to have applied transplantation of full-thickness grafts on deeply dissected recipient corneas (Hallermann, 1959). Removing the entire stroma while baring DM and endothelium proved to be beneficial in terms of visual outcome. Additionally, full-thickness grafts were altered by being disposed of DM and endothelium.

In the course of time, several deep anterior lamellar keratoplasty (DALK) techniques were developed, mainly targeting facilitation of separation of stroma from DM, as it arguably represents the most challenging part of the operation (Melles et al., 1999). An overview of different DALK techniques is reported in 1.4.3.

Nowadays, the preferred approach is to create an initial cleavage between stroma and DM, prior to removal of the host stroma. This is performed by injection of viscoelastic ("visco-delamination", Melles et al., 2009) or air into the pre-Descemet plane. The latter corresponds to "Big-bubble"-DALK[34], which will be explained in detail in 1.4.

1.3.4.2 Development of posterior lamellar keratoplasty techniques

Lamellar transplantation targeting posterior corneal tissue is a relatively new approach, with first attempts performed in the 1950s by Barraquer and Tillett (Güell et al., 2014). Target structures initially comprised posterior stroma along with endothelium and DM, as selective excision was not yet technically possible. Posterior tissue was manipulated and transplanted below a sutured stromal flap, which mostly resulted in poor postoperative outcome (Barraquer, 1950).

In the 1990s, endothelium and DM could be targeted more precisely, as instruments and microscopes advanced. Descemet stripping (automated) endothelial keratoplasty (DSEK/DSAEK) technique evolved, in which the DM was "stripped off" the stroma (Dapena et al., 2009; Gorovy, 2005). Donor tissue was inserted into the anterior chamber through limbal incisions and held in place by an air bubble instead of sutures. The technique was further perfected by Melles et al. in 2006 into Descemet Membrane endothelial keratoplasty (DMEK), which is enables selectively targeting endothelium and DM (Melles, 2006). DMEK is today's gold standard procedure for endothelial keratoplasty.

1.4 DALK

1.4.1 Purpose of DALK

DALK is a lamellar transplantation technique utilized to remove and replace all corneal layers anterior to the DM. The procedure aims to cause a dissection between the deep stromal layer and the DM, with subsequent removal of the whole stroma along with the BL and epithelium (Anwar & Teichmann, 2002). Ideally, the DM should be left fully bare without residual stroma, as this has been shown to be associated with significantly better

outcome in best-corrected visual acuity (Reinhart, 2011). The donor graft is disposed of endothelium and DM and sutured in place of the removed tissue.

1.4.2 Indications for DALK

Indications for DALK encompass diseases where the host's DM and endothelium are intact and functional, but the layers anterior to the DM are defected or diseased.

Most commonly, it is used for treatment of advanced keratoconus, in which progressive thinning and steepening of the cornea causes visually relevant astigmatism. Patients who develop a visually relevant Keratoconus are oftentimes diagnosed at a young age. Their endothelium and DM are typically healthy (Karimian & Feizi, 2010).

Another typical indication is Pellucid marginal degeneration, a disease which is characterized by crescent-shaped thinning in the inferior periphery of the cornea. It is the second most common non-inflammatory cause for corneal thinning after Keratoconus (Sridhar, 2004). Again, DM and endothelium in these patients are typically healthy.

Further indications include iatrogenic corneal ectasia such as post-refractive surgery corneal ectasia, dystrophies limited to the corneal stroma, as well as scars or opacity reaching deep into the stroma while not comprising the integrity of the DM or endothelium (Nanavaty et al., 2018).

1.4.3 Overview of DALK techniques

The clean dissection of stroma and DM arguably represents the most difficult step in DALK, as it frequently results in perforation. Several techniques have thus been suggested that aim to facilitate the dissection.

In 1984, Archila proposed intrastromal air injection to aid dissection (Archila, 1984). In a study by Sugita in 1997, DALK was performed by hydro-dissection, involving injection of a saline solution (Sugita & Kondo, 1997).

As described in *1.4.3.1*, today's commonly used methods aim for detachment of stroma by rather deep injection, targeting the pre-Descemet plane. As for injection substance, use of viscoelastic was proposed by Melles in 1999. In 2002, Anwar et al. introduced the Big-Bubble technique, in which air is injected. Both are arguably today's leading techniques in DALK. Big-Bubble DALK will be introduced in 1.4.4.

1.4.4 Big-Bubble DALK

1.4.4.1 Objective

Published in 2002 by Anwar et al., the technique is aimed to facilitate clean dissection of the host's corneal stroma from DM by injecting air into the pre-Descemet plane, creating a cleavage between the two structures. That way, removal of stroma is facilitated. Nowadays, Big-Bubble DALK is arguably the most commonly used technique for anterior lamellar keratoplasty (Goweida et al., 2020).

In *1.4.4.2*, the procedure is explained in detail as originally described by Anwar & Teichmann in 2002. It is important to mention that modifications of the technique have been developed in recent years, for example involving femto-laser excision (see *1.4.4.5*). Some modified versions are frequently in use today.

1.4.4.2 Big-Bubble technique in detail

Initially, the patient's cornea is trephined to a depth of 60 – 80%, so a central button is created. The usage of a calibrated trephine system is recommended. Manual deepening of the initial trephine groove can be performed if considered too shallow.

A 27- or 30-gauge cannula is attached to a 1ml to 3ml air-filled syringe. It is bent manually approximately 5.0 mm from its tip, so the terminal and proximal segment of the cannula comprise an angle of approximately 60 degrees. The bevel should be facing down.

Paracentral insertion of the cannula into the corneal button is performed at a convenient entry side, bevel facing down. It is then carefully advanced into the stroma, following an oblique direction, tangentially approaching the cornea's central area. Advancement up to the very center is avoided, as it is generally the thinnest area.

The tip of the cannula is desired to reach deep into the stroma, while forming an air-tight tunnel within the stroma. To reach the pre-Descemet plane and enable stromal detachment, it is suggested that air-injection is aimed at sufficient depth. A recent study by Patricha et al. found that a depth traversing at least 79.9% of the corneal thickness significantly increased the probability of successful pneumo-dissection. Depths greater than 90% however are not believed to be necessary (Pasricha et al., 2016).

Once the desired depth is reached, air injection is performed by carefully pressing the plunger of the air-filled syringe. The desired effect is the formation of a large bubble between the deep stroma and the DM. Its successful formation is indicated by the sudden appearance of a "white, semi-opaque disk", which in most cases does not extend to the trephine groove. Its outline should be approximately circular. The event is accompanied by a sudden easing of resistance of the plunger. If this result is observed, pressure on the plunger should be released, and the cannula withdrawn.

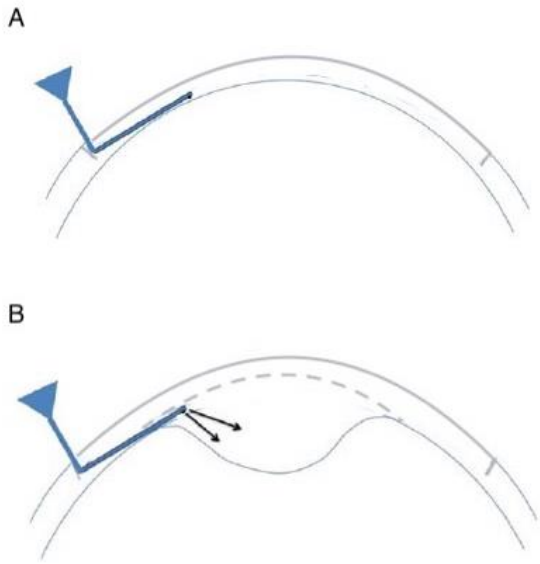

Illustration 4. **Pneumo-dissection by air injection in Big-Bubble DALK.**
A: Placement of cannula in deep stromal tissue.
B: Big bubble formation between stroma (dotted line) and Descemet Membrane (continuous line) after air-injection. [Image source: F4, modified]

In the event of the desired big bubble formation, successful detachment of the stroma from the DM can be presumed (see *Illustration 4*). Anterior keratectomy can subsequently be performed while baring a thin stromal layer anterior to the created bubble first. Following the initial keratectomy, the eye may be softened by draining intraocular fluid through a paracentesis prior to removing the remaining stroma. Provided pneumo-dissection was successful, no firm adhesions are expected to remain on DM, which allows for clean removal of the entire stroma.

After complete removal of the corneal button, the donor graft is prepared by disposal of DM and endothelium. It is placed onto the host's DM and secured by sutures.

It is important to mention that Anwar in his publication suggests cannula insertion under direct visual control. However, nowadays, DALK is generally performed using a surgical microscope. Therefore, it was also used for the simulations in the scope of this work (see *2.1.2.1*).

1.4.4.3 Postoperative outcome compared to PKP

DALK has been shown to be associated with significantly less endothelial graft rejection and thus, on average, longer transplant durability as compared to PKP (Reddy et al., 2015). Graft rejections in PKP are known to derive from endothelial cell rejection most commonly, accounting for 50% of rejections (Guilbert et al., 2013). As successful DALK preserves the host endothelium and DM, the possibility of endothelial rejection is therefore eliminated (Warson et al., 2006).

Stromal and epithelial rejection is observed in 8-10% of patients, however generally rejection rate is significantly lower as compared to PKP (Watson et al., 2004), with less than 5% graft failure secondary to rejection. A lower quality graft is usually better tolerated following DALK rather than PKP (Schaub et al., 2017).

Secondary glaucoma and secondary cataract have been observed less frequently in DALK compared to PKP (Liu et al., 2015), as ideally, the anterior chamber remains uncompromised in successful DALK.

Outcomes in best-corrected visual acuity and graft clarity in unrejected grafts following DALK have been shown to be comparable to those following PKP (Sari et al., 2012). However, stromal residue following DALK was reported to affect visual outcomes negatively (Tan et al., 2010).

1.4.4.4 Intraoperative complications

As described in *1.4.4.2*, precise air injection at a sufficient depth is crucial to achieve a clean pneumo-dissection. The latter is necessary to avoid any residual host stroma after DALK, as post-operative haze or opacification can occur, leading to limitation of visual acuity (Ardjomand et al., 2007). Prognosis is considered best when baring of the naked DM is successful.

Following recent studies, reaching a depth traversing at least 79.9% of the corneal stroma thickness, or greater, is recommended to achieve a bare DM.

Naturally, aiming for deep stromal layers bears higher risk of DM perforation, which is indeed the most common intraoperative complication. It typically leads to intraoperative conversion to PKP; however, it remains an individual decision based on the intraoperative status.

Perforation rates are mostly reported to range from 7% to 30% of operations (Jhanji et al., 2010;, Huang et al., 2019; Ozmen et al., 2018; Kodavoor et al., 2022; Kocluk et al., 2017). Some studies report conversions to PKP due to DM perforation as high as 42.5% (Kocluk et al., 2017). Albeit the use of a sharp cannula is recommended for insertion into the corneal stroma, it increases the chance of puncturing DM when inserted too forcefully. Furthermore, with advanced keratoconus being the most common indication for DALK, host corneas are typically thin and thus, conceivably more difficult to manipulate without perforation. Perforation may also be caused by excessive air injection or too forceful injection (Jhanji et al., 2010).

Completed DALK following (micro-)perforation can lead to postoperative complications, such as secondary glaucoma or cataract (Kodavoor & Dandapani, 2022). A less common event is a so-called double anterior chamber, which occurs when DM and stroma form a space separated by aqueous humor (Fournié et al., 2007).

All factors considered, DALK is a technically demanding procedure, resulting in a relatively high failure rate.

1.4.4.5 Modifications

Responding to DALKs high intraoperative complication rates, the technique has frequently been modified to increase safety and improve success rates.

Modifications include performance of keratectomy prior to cannula insertion and air-injection into the remaining stroma, which has shown to better success rates in some studies (Fogla, 2013). Further work suggests pre-formation of a stromal nick prior to insertion of a blunt cannula for subsequent air injection (Fournié et al., 2007). It is presumed that thereby, probability of puncturing DM during air injection decreases.

Femtosecond laser excision has been used for calculated, precise trephination and pre-formation of stromal pockets, eliminating the possibility of perforation by needle or cannula (Alio et al., 2015). Recent research suggests that air injection following laser-cut stromal tunnels increase the possibility of successful Big-Bubble formation (Malyugin et al., 2023).

1.4.4.6 Perioperative and intraoperative imaging

Attempts to facilitate DALK included implementation of imaging techniques. The development of Optical Coherence Tomography (OCT) in 1997 enabled non-invasive cross-section imaging of ocular structures. The system underwent steady improvement and made anterior segment visualization possible in 2006. Newer generation models are used for biometric measures such as corneal topography, tomography, and calculation of intraocular lens implants. Nowadays, the examined tissue can be visualized on a histological scale up to micrometer resolution (Gabriele et al., 2011). Potential benefits of implementing OCT during ophthalmic surgical procedures have oftentimes been considered and investigated (Maier et al., 2018).

It is conceivable that imaging of corneal layers and instrument localization throughout DALK may be beneficial. It may help assess the relative depth of the cannula tip and thus facilitate reaching a sufficient depth while avoiding perforation.

Many studies have implemented intraoperative OCT imaging during DALK to provide critical information to the surgeon (Steven et al., 2014). Both static intraoperative captures

and real-time OCT have been used for this purpose. It is generally agreed upon that intraoperative OCT imaging may contribute to better surgical outcomes (Steven et al., 2014; Au et al., 2015). For instance, depth assessment may be facilitated and thus, a too shallow cannula placement identified (Santorum et al., 2022).

1.5 Objective of this work

In recent years, DALK has been shown to be an excellent alternative to PKP in treatment of keratoconus and other corneal diseases in patients with healthy DM and endothelium. Surgical outcome has been shown to be superior to PKP regarding postoperative complications and graft durability. Potential endothelial graft rejection is eliminated in successful DALK, while epithelial or subepithelial graft rejection occurs significantly less frequently. At the same time, postoperative visual acuity has shown to be comparable in DALK and PKP.

However, DALK is a challenging operation with relatively high intraoperative failure rates even when performed by experienced surgeons. The procedure is arguably difficult to learn and may result in a lot of “trial-and-error”. Most commonly, failure occurs due to DM perforation.

Efforts have been made to facilitate DALK which, to some degree, have resulted in making the procedure safer and lower failure rates. Intraoperative OCT-imaging has been shown to be a promising approach, aiding the surgeon by providing information on instrument localization and relative depth assessment of the cornea.

To further improve success rates in Big-Bubble DALK, it is conceivable that robotic assistance may be beneficial. Naturally, it may eliminate hand-tremor and the need for accurate hand-eye-coordination. This, in turn, may steepen the learning curve in novice

surgeons. It may furthermore be beneficial for the patient, as it may increase precision and thus, increase the likelihood of Big-Bubble formation, as greater depths can be achieved.

The objective of this work is to investigate potential facilitation of Big-Bubble DALK by implementing robotic assistance coupled with real-time intraoperative OCT-imaging. For this purpose, cannula insertion followed by air injection was performed on porcine eyes under an ophthalmic microscope with and without robotic assistance. Real-time intraoperative OCT monitoring was implemented throughout both settings, providing information on corneal depth and instrument localization throughout trials.

In 2020, Draelos et al. published an equivalent study, in which a combined system of robotic assistance and intraoperative OCT was utilized during cannula insertion in human cadaver corneas[89]. This setup was compared to manual insertion without any imaging modality. Draelos et al. (2020) reported a significant increase in achieved depth without perforation using the cooperative system compared to manual insertion.

As opposed to the approach by Draelos et al. (2020), in this work, intraoperative OCT was implemented throughout both settings, thus specifically comparing outcomes of robot-assisted and manual performance under intraoperative OCT. Furthermore, air injection followed cannula insertion, provided no perforation occurred. Corneas were examined prior to and following air injection. Simulations were performed on porcine instead of human cadaver eyes.

A custom-made robot was implemented for assisted trials. All trials were performed using a surgical microscope equipped with real-time intraoperative OCT. Visual feedback for instrument localization and depth information were provided to the surgeon throughout all trials. Performance was evaluated for each setting and results were compared.

2. METHODS

Followingly, methods used for the scope of this work will be specified as published in the article Comparison of Robot-Assisted and Manual Cannula Insertion in Simulated Big-Bubble Deep Anterior Lamellar Keratoplasty by Zhao, Jablonka, Maierhofer et al. in 2023.

2.1 Material

2.1.1 Porcine eyes

Porcine eyes were obtained from a local slaughterhouse and used for the experiments within 3 hours after collection. The eyes were extracted using a technique that kept the bulbus and especially the cornea uncompromised. All eyes were checked for corneal damage or haze prior to including them in the experiments.

After collection and in between experiments, eyes were stored in a glass container filled with balanced salt solution (BSS) to prevent corneas and adnexal conjunctive tissue from drying and thus maintain elasticity.

2.1.2 Devices

2.1.2.1 Microscope and intraoperative OCT

All experiments were performed using a standard ophthalmic surgery microscope equipped with an OCT engine, capable of sharing the same optical path with the microscopic view (LUMERA 700 with RESCAN 700, Carl Zeiss Meditec, München, Germany). Two OCT planes, i.e., B-scans are continuously captured by the OCT engine as to generate a real-time

tomography of the examined tissue. Alignment of the B-scans onto the desired location within the vertical and horizontal plane were carried out by the surgeon using a foot control pedal or by the assistant using the auxiliary screen. The surgical field was directly observed through the microscope's ocular with the OCT acquisition location marker overlaid onto the scene (*Illustration 5*).

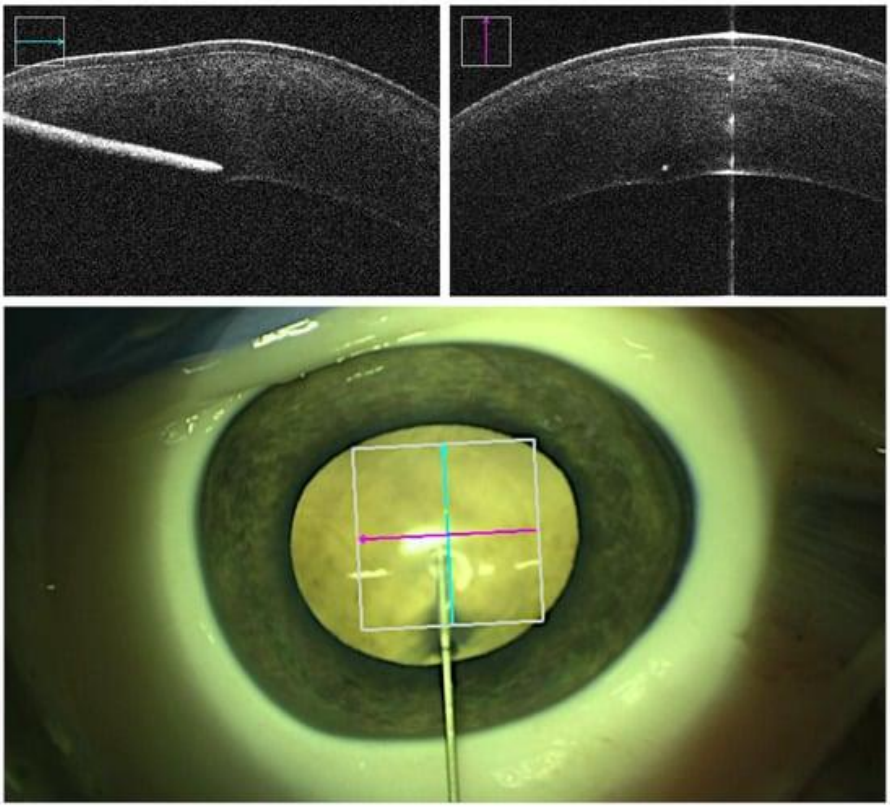

Illustration 5. **OCT B-Scan acquisitions (top) and the microscopic view (bottom) of cornea and cannula during a robot-assisted trial.**

B-Scan capture locations are indicated by cyan and magenta arrows. [Image source: F5]

The B-Scans were aligned so that tomography of the cornea along with cannula tomography was possible. Localization of the cannula relative to the tissue was assessable.

Recording of image and video material (microscopic field view and OCT-acquisition) was available.

2.1.2.2 Robot

The robot uses a hybrid parallel–serial system with prismatic piezo actuators. Its three limbs are interconnected by two joints, whose combined movement controls the alignment of the robot's effectuating limb. The latter is mounted with the utilized instrument; in this setting, an air-filled syringe tipped with a cannula. Movement comprises five degrees of freedom, allowing the alignment of the effectuating limb with the attached instrument to a precision of 10 microns.

The air-filled syringe tipped with the cannula was mounted onto the effectuating limb of the robot. It was controlled in a master–slave fashion using a 3D mouse, regulating the desired orientation of the instrument respecting the cannula tip as the center of motion.

The working volume of the robot approximated a perfect sphere with a radius of 30 mm; this working volume covered the entire corneal surface area and corneal depth with prior appropriate placement of the robot. Movement of the robot was subject to a velocity control system, which allowed for a steady motion of the tool.

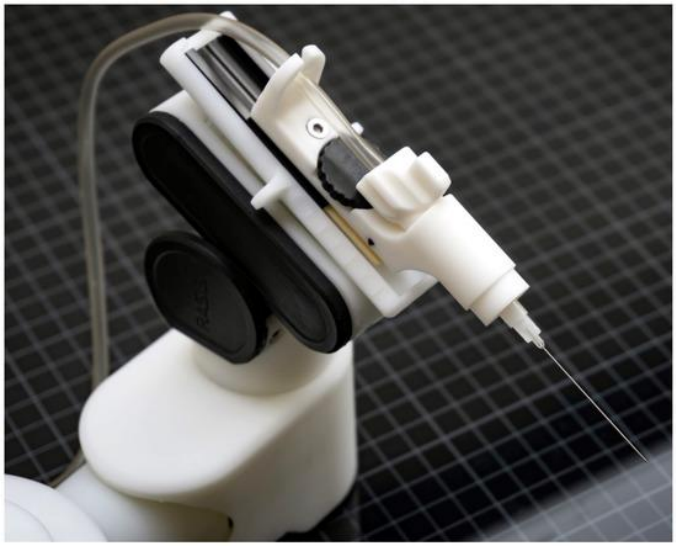

Illustration 6: **Custom-made robot holding injection cannula.**

The cannula is attached to an extension cable, extending from an air-filled syringe (not shown in the image). [Image source: F6]

2.1.3 Instruments

Both manual and robot-assisted trials were conducted using a 1 mL syringe filled with approximately 0,8 ml of air. It was tipped with a disposable sharp 12 mm long 30-gauge cannula. In robot-assisted trials, the syringe was mounted onto the robot.

2.2 Experimental setting

2.2.1 Task

The task was to perform DALK cannula insertion into the porcine corneal stroma while aiming for a depth of at least 80%, as this has been shown to correlate with a higher probability of success[61]. Perforation shall be avoided. Intraoperative OCT could always be used to localize cannula tip relative to the corneal tissue.

At a depth considered sufficient, air injection was performed, aiming for big bubble formation between deep corneal stroma and DM.

One half of the trials was performed manually, the other half was performed by robotic assistance. Operators were two novice surgeons with no prior experience in clinical or experimental ophthalmic surgery. Beforehand, they received minimal training by verbal instructions and supervision from an experienced ophthalmic surgeon.

Operators were randomly assigned to trial order and fashion, namely manual or robot assisted. The other operator, respectively, assumed the assistant role to maneuver OCT imaging. Randomization was intended to potentially minimize bias due to learning effects.

Intraoperative OCT was enabled and focused by the assistant so both the corneal stroma and the cannula were displayed in cross- and longitudinal sections. The cannula was then aligned following the intended insertion angle relative to the corneal central surface. The alignment was realized by remote-controlled fine adjustments continuously carried out by the assistant. Insertion was executed aiming for an estimated depth of 80% or greater while taking care to

avoid penetration into the DM. Depth information was continuously obtained from projected real-time intraoperative OCT images and, on inquiry, confirmed or reevaluated by the assistant. At the desired depth, air injection was performed, and formation of the demarcation plane was observed and recorded.

2.2.2 Preparation

Before each trial, porcine eyes were checked for physical integrity and clear cornea.

To secure porcine eyes throughout the procedure, a rubber base imitating the orbit was used. Eyes were fixed by pins puncturing the lateral conjunctive tissue and adhering it onto the base. This allowed for passive movements simulating elevation and depression along the transversal axis.

To control for intraocular pressure, a 23-gauge trocar was implanted approximately 3.0 – 4.0 mm from the limbus and connected to an infusion system. Homogenous pressurization of the bulb to around 20 mmHg was ensured by passive infusion of balanced salt solution into the vitreous cavity, regulated by bottle height.

The surgical microscope (see 2.1.2) was placed above the eye. Magnification and focus were set until convenient. OCT focus was automatically aligned with microscope focus. The syringe utilized in the trials was air-filled until approximately 0,8 – 1 ml, to ensure sufficient volume.

In robot-assisted trials, the air-filled syringe was mounted onto the robotic arm. The system was then calibrated minding the cannula tip as initial reference point. Followingly, the robot was placed so the tip of the 30-gauge cannula was located within 1-2 cm of anticipated insertion, that way ensuring full range of motion. The 3D mouse for remote control was placed within comfortable reach for the surgeon.

In manual trials, the cannula was bent 60 degrees for better ergonomic handling, corresponding to the state of the art. In robotic trials, bending of the cannula was not necessary, as no effect on ergonomics would have been achieved.

2.2.3 Trial execution

After gentle manual check for sufficient intraocular pressure, a cannula entry point at approximately 6h was determined. It was aimed to enter close to the limbus, so to ensure sufficient tunnel length.

OCT B-Scans were aligned either by the surgeon using a foot pedal, or, by the assistant using the auxiliary monitor. The alignment of the B-Scans was aimed to display continuously display the cannula in cross- and longitudinal section, thus providing real-time cannula localization relative to the stroma.

Under intraoperative OCT monitoring, cannula insertion was performed with a 30-gauge cannula, with the beveled side facing towards the DM.

Insertion was aiming towards the central area of the cornea under OCT monitoring. Proper alignment of the OCT B-Scans was ensured by steady adjustment of the scans throughout the procedure. Depth information was continuously obtained from image projection onto the surgical field observed through the microscope.

Once the cannula tip was placed at the desired depth, air was injected into the deep corneal stroma and then, the cannula retracted.

In clinical procedures, if big-bubble formation succeeds, the operation is finalized by removal of stroma anterior to the DM and replacement of the tissue by a donor graft. These steps were not carried out in this experimental setting.

2.3 Hypotheses and parameters

It was investigated whether robotic or manual setting would show significant differences in 1. mean achieved depth, 2. success and failure rate, 3. cannula entry angle and 4. stromal tunnel length.

Throughout all trials, real-time intraoperative OCT and microscopic visual field were recorded. Three-dimensional OCT volumes of the cannula tip and the corneal stroma were captured at multiple critical events: 1) prior to cannula insertion, 2) prior to air injection at the desired depth, 3) post-air injection, displaying demarcation plane in the deep stroma in successful trials (representative of potential successful bubble formation), 4) post-retrieval of cannula, displaying the stromal tunnel caused by the cannula. This allowed for postoperative analysis of the trial outcomes.

2.3.1 Mean achieved depth

Manual versus robotic-assisted trials were evaluated regarding mean achieved depth. Achieved depth was calculated by postoperative evaluation of OCT 3D-volumetric captures which were acquisitioned prior to air injection. In these captures, the cannula tip is located at the deepest position throughout the procedure. Mean achieved depth is specified in percentage of total corneal thickness. Calculation was aided by a software designed by Zeiss Meditec for experimental purposes.

2.3.2 Success and failure rate

Success or failure was determined based on 1. whether perforation of DM occurred and 2. outcome regarding big-bubble formation.

Trials were considered failed when 1. perforation of DM occurred at any point throughout the trial. Puncturing of the DM by the cannula tip was either observed directly in OCT or it was

deferred by definite indicators. Indicators were visible air bubbles below the corneal surface due to air leakage through the DM, or discontinuity of the DM visible in the OCT, or both. Trials were furthermore considered failed when 2. no big bubble could be achieved after air injection. This was indicated when the demarcation plane was displayed in the superficial rather than deep corneal layers. Smaller intrastromal air bubbles would then form a dense, cloudy layer just below the epithelium (see *Illustration 7*). As intrastromal air causes OCT rays to be reflected, no details in greater corneal depth could be visualized below the superficial bubbles. In total, unsuccessful air injection was clearly discernable from the desired pre-descemetal demarcation.

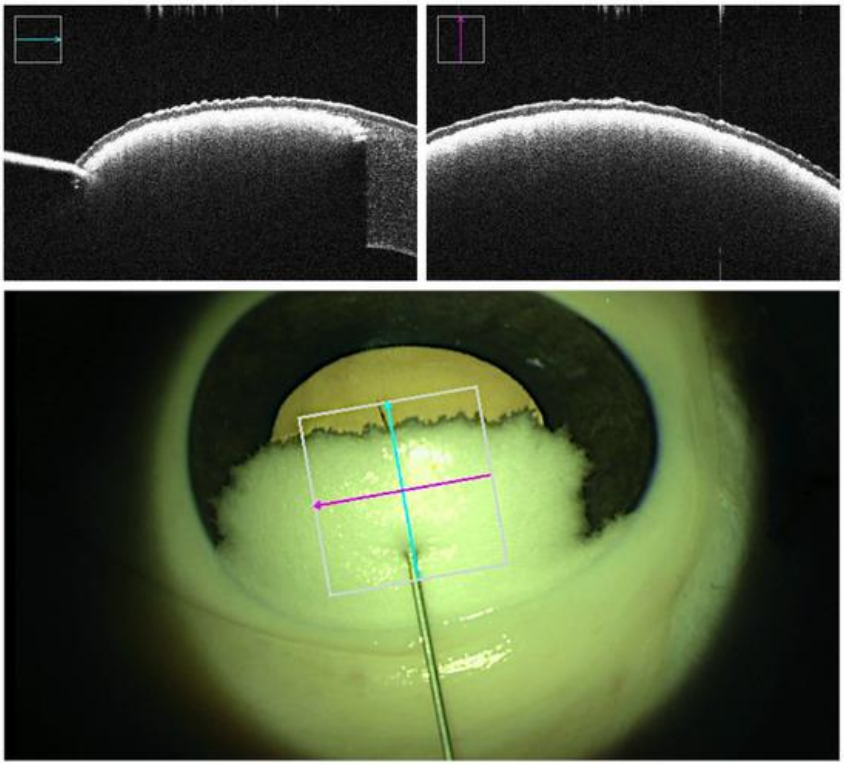

Illustration 7. **An example of unsuccessful bubble formation following air injection.** OCT acquisitions (top) and the microscopic view (bottom) show small bubble formation in the superficial cornea, appearing as a cloudy layer directly below the corneal epithelium. Cyan and magenta arrows indicate OCT capture locations. [Image source: F7]

In turn, bubble formation was considered successful when the injected air caused a sharp, homogenous demarcation layer right above the DM. In these cases, no air was penetrating more superficially located stromal layers (see *Illustration 8*).

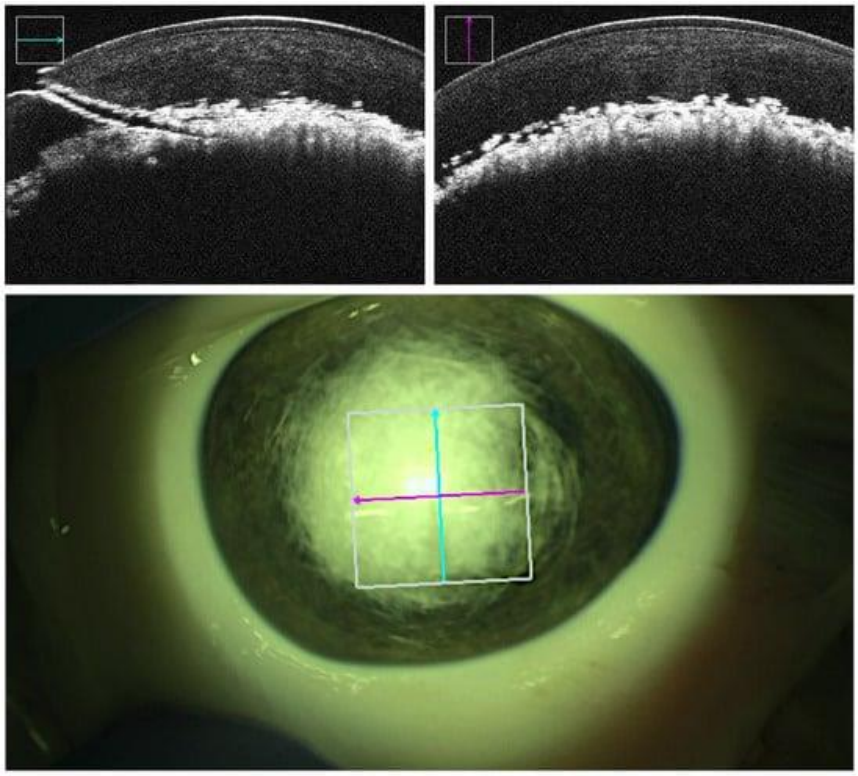

Illustration 8. **Example of successful deep air injection.**

OCT acquisitions (top) and microscopic view (bottom) show a deep demarcation layer, with no air present in the superficial cornea. The stromal tunnel formed by the cannula is visible in the OCT B-scan captured along the cannula trajectory after its retraction. Cyan and magenta arrows indicate capture location. [Image source: F8]

It is important to note that the physical detachment of the DM could not be reproduced, as rearing pigs are typically young at the age of slaughter. Thus, the tissue is still quite immature and thus, adhesion between the DM and stroma is stronger (Zeng et al., 2001).

2.3.3 Cannula entry angle

Cannula entry angle refers to the angle between the longitudinal section of the cannula in relation to the central corneal surface. For its analysis, OCT scans were captured immediately prior to insertion, when the desired cannula orientation was set. The scans' analyses were carried out using a software developed by Zeiss Meditec for experimental purposes.

2.3.4 Stromal tunnel length

The stromal tunnel is created by the sharp tip of the cannula as it is inserted forward. Tunnel length is measured by software-based analysis of OCT scans that display the stromal tunnel post-retraction. It is measured in both successful and unsuccessful trials, for manual and robotic trials respectively.

3. RESULTS

Followingly, results of the simulations performed in the scope of this work will be specified as published in the article *Comparison of Robot-Assisted and Manual Cannula Insertion in Simulated Big-Bubble Deep Anterior Lamellar Keratoplasty* by Zhao, Jablonka, Maierhofer et al. in 2023.

3.1 Overview

Simulations were performed on 48 ex vivo porcine eyes in total, with half of them performed manually and the other half performed by robotic assistance. Measurements were calculated by analysis of OCT captures, aided by a calculation software.

The mean corneal thickness was 998 microns with a standard deviation of 10 microns. Due to low intraocular pressure in two eyes despite intravitreal infusion, only 46 trials, half manual and half robot-assisted, were included in the evaluation.

An average volume of 0.24 mL of air was injected in all cases in which perforation had not occurred prior to reaching the desired depth.

3.2 Outcome

3.2.1 Success and failure rates

In total, 74% of manual compared to 83% of the robotic trials were successful. 26% of the manual trials failed, while 17% of the robotic trials failed. Perforation of the DM accounted for three failures in manual trials, when in robotic trials, only one perforation occurred.

Failure due to insufficiently deep demarcation layer, i.e., successful bubble formation was present in both settings.

Both the differences in success rates and in perforation rates in robotic and manual trials were not significant (two-tail t-test with significance of $p < 0.01$). Success and failure rates are shown in *Table 1*.

		Successful Manual (74%)	Failed Manual (26%)	Successful Robotic (83%)	Failed Robotic (17%)
Achieved depth (stromal percentage)	Mean	85.05%		89.29%	
	STD	4.52%		4.03%	
Cannula entry angle (degree)	Mean	23.45°	28.61°	23.35°	32.44°
	STD	8.80°	9.13°	6.48°	5.73°
Stromal tunnel length (millimeters)	Mean	1.82 mm		1.72 mm	
	STD	0.27 mm		0.45 mm	
Operation duration (seconds)	Mean	212 s		260 s	
	STD	96 s		96 s	

Table 1. **Means with standard deviations of the measured parameters in robotic and manual trials.**

3.2.2 Achieved depth

Mean achieved depth in successful cases was greater in robotic trials (89.29% of the cornea with a standard deviation of 4.01%) than in manual trials (85.05% of the cornea with a standard deviation of 4.52%). This difference was significant ($p < 0.01$, independent samples t-test). Achieved depths are plotted in *Table 2*.

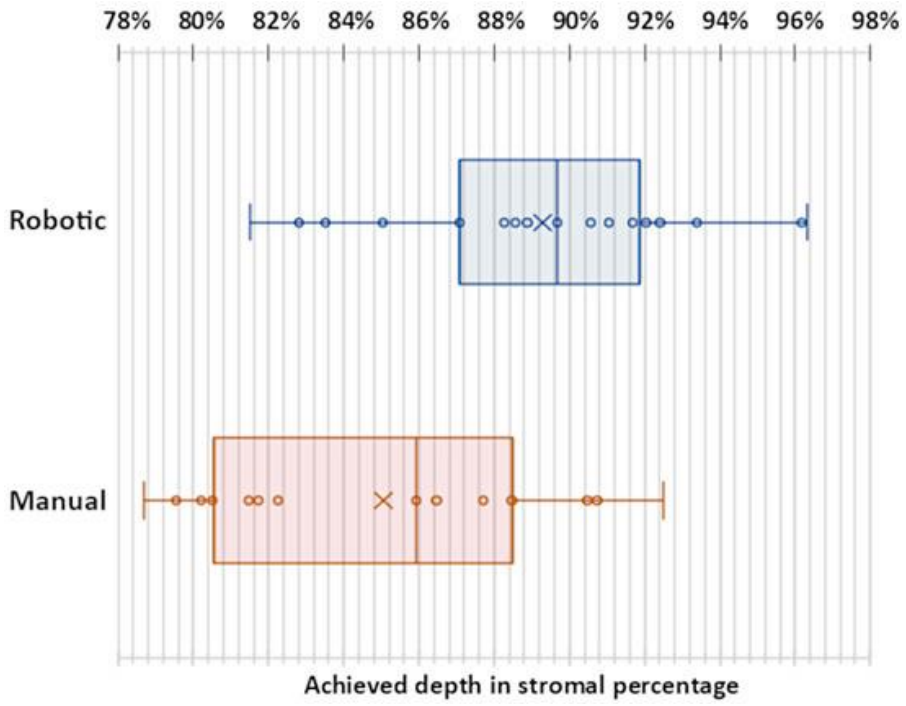

Table 2. **Box plot showing achieved depth in successful trials for robot-assisted (blue) and manual (red) trials.**

Mean depth is indicated by cross, median depth indicated by vertical band. [Image source: F10]

3.2.3 Cannula entry angle

The mean needle entry angle in successful manual trials was 23.45 degrees (STD: 8.80 degrees); in successful robotic trials it was 23.35 degrees (STD: 6.48 degrees). This was opposed to entry angles of 28.61 (STD: 9.13) degrees in manual trials and 32.44 (STD: 5.73) degrees in robotic trials (see *Illustration 9*). Successful trials were shown to more often follow a flatter insertion angle whereas unsuccessful trials were shown to more often follow a steeper insertion angle. *Illustration 9* displays OCT captures utilized for insertion angle calculation.

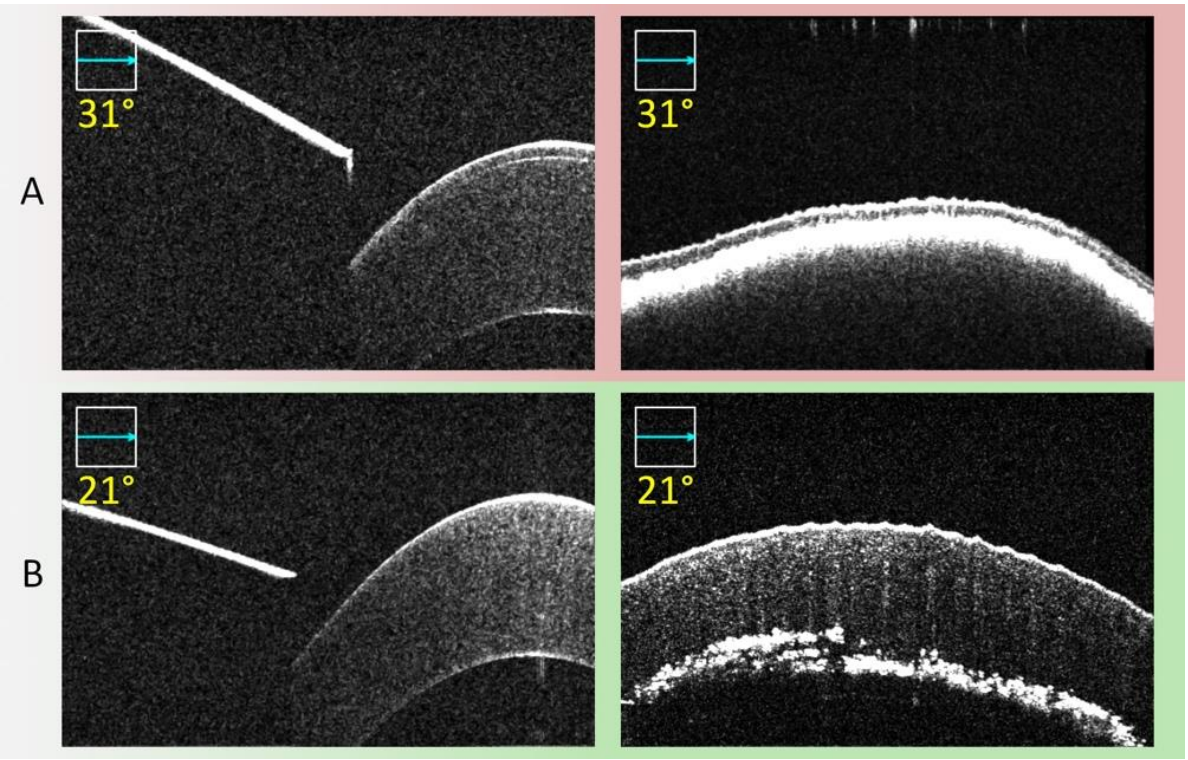

Illustration 9. **Examples of OCT-acquisitions of cannula entry angle relative to the cornea's central surface.**

Following an insertion angle of 31 degrees (top), a superficial air deposition was observed. Following an insertion angle of 21 degrees (bottom), a deep demarcation layer, indicating successful big bubble formation, was visible. [Image source: F11]

3.2.4 Stromal tunnel length

The mean tunnel length in successful trials was 1.76 mm with a standard deviation of 0.38 mm. The induced tunnel in robotic trials (mean 1.72 mm, standard deviation 0.45 mm) differed from manual trials (mean 1.82 mm, standard deviation 0.27 mm), however not significantly. Mean tunnel length in successful and unsuccessful trials were similar (for

robotic trials, 1.72 mm, and 1.71 mm respectively; for manual trials, 1.82 mm, and 1.88 mm respectively).

Mean stromal tunnel lengths are shown in *Table 1*.

3.2.5 Operation duration

The mean duration of the operations in successful trials performed with robot assistance was 261 s with a standard deviation of 96 s, which was considerably longer than in successful manual trials, at 212 s with a standard deviation of 96 s. Surgical time did not include robot preparations and calibrations. Operation duration time is indicated in *Table 1*.

4. DISCUSSION

4.1 Summary of results

This work could show that novice surgeons with no prior experience in ophthalmic surgery could generate an airtight tunnel in the porcine cornea. They could do so in both, manual and robot-assisted setting while monitoring depth information and instrument localization with real-time intraoperative OCT. Success rates were 74% with manual performance and 83% with robotic performance, which is largely consistent with statistics in clinical practice (Jhanji et al., 2010). However, success and failure rates vary among studies and appear to largely depend on the chosen technique and the surgeon's expertise.

In both settings, a depth exceeding 79% of the cornea was reached, which has shown to increase the probability of resulting in big bubble formation (Pasricha et al., 2016). Following cannula insertion, air injection, in most cases, resulted in the generation of a sharp, deep stromal demarcation plane, representative of successful big bubble formation.

In successful trials, a significantly greater depth could be achieved with robotic assistance than in trials performed manually.

Successful trials seemed to follow a shallower insertion angle, while failed trials followed a steeper insertion angle. Tunnel length was slightly longer in robotic trials, however not significantly.

Operation duration of successful trials was longer in robotic trials than in manual trials, not considering the calibration and set up time.

4.2 Potential implications

4.2.1 Intraoperative imaging by real-time OCT

It is feasible that information on tissue depth and instrument localization is beneficial for DALK, as in this study, novice surgeons were able to complete cannula insertion and air injection with an arguably low failure rate, both in manual and robotic trials. A possible benefit in terms of safety and successful outcome was assumed following various studies, in which DALK was performed under iOCT (Steven et al., 2014; Au et al., 2015; De Benito-Llopis et al., 2014).

As already mentioned in 1.5, Draelos et al. (2020) published an experimental study investigating the effect of a cooperative system, consisting of intraoperative OCT and robot-assisted cannula insertion. Equivalent to our approach, inexperienced surgeons performed cannula insertions using robotic aid coupled with intraoperative OCT, however their simulations were conducted on human cadaver eyes, and manual trials were not accompanied by intraoperative OCT imaging. Trials performed with the cooperative system were shown to have lower perforation rates as opposed to manually performed insertion, albeit conducted by inexperienced individuals.

These results allow to speculate that novice surgeons, due to lack of experience, may have trouble estimating the location of the cannula tip inside the stroma throughout the procedure. Thus, it is conceivable that better outcome may be expected with intraoperative OCT, since reasonably accurate real-time information on cannula tip location is provided and may balance lack of practice.

4.2.2 Robotic assistance

Robot-assisted trials were shown to reach a significantly greater depth than manually performed trials. This is consistent with the findings by Draelos et al. (2020), who showed an increase of achieved depth by 31% when performed with robotic assistance and intraoperative OCT, as opposed to manual performance without any means of imaging (Draelos et al., 2018). In their study, a mean depth of 71% was reported using the cooperative system; in our study, a greater average depth of 89% was achieved by robotic assistance (Zhao et al., 2023). Regarding these findings, it is conceivable that the application of intraoperative OCT coupled with robotic assistance may contribute to a more precise cannula insertion, sufficient depth and thus, successful big-bubble formation. This may lessen the numbers of conversion to PKP, which in turn is beneficial for the patient, it decreases surgery time and therefore, environmental exposure of the tissue. Due to this, probability of infection may be lower.

Novice surgeons may benefit from using imaging to get acquainted with the technique, while keeping perforation rates low and thus possibly achieve higher success rates.

In the study by Draelos et al. (2020), air injection did not follow cannula insertion, meaning that there was no clear indicator whether bubble formation was going to be successful despite sufficient depth. In our study however, all cases in which no previous perforation occurred were followed by air injection with a subsequent analysis of the air deposits within the stroma. Deep air deposits causing a sharp demarcation above the DM were considered indications for successful big bubble formation and were proving the stromal tunnel to be airtight. If the air deposits were displayed in superficial corneal layers, the trial was considered a failure and was thus not included in the mean achieved depth calculation. It is important to note, however, that DM detachment was not visible in OCT despite a deep air deposit (see *Illustration 8*). This concurred with previous observation in porcine models, as

porcine eyes at the usually young slaughtering age show strong adhesion between corneal layers (Guo et al., 2020).

As mentioned above, in non-perforated cases, a mean depth of 89% by robotic aid and 85% in manual trials could be achieved. As shown by Pasricha et al. (2016), achieved depths of greater than 79% likely result in successful Big-Bubble formation. Thus, the mean depths reached in this study could be considered sufficient to assume a high probability of successful pneumo-dissection.

Pasricha et al. (2016) also reported that depths surpassing 90% were not conditional for successful pneumo-dissection. However, depths up to 96% were reached in robotic trials without causing perforation. It is conceivable that incorporating robotic assistance in DALK or similar ophthalmic procedures may increase accuracy and thus have a positive impact on outcome. Increased accuracy may be achieved due to steadiness of motion during insertion, better ergonomics, and the elimination of hand tremor.

As stated in *1.4.4.3,* DALK shows numerous benefits over PKP, but comes at the cost of a high failure rate even in experienced hands. It is also associated with an increased operation time compared to conventional penetrating keratoplasty (Modabber et al., 2023). As conversion rates are high, corneal surgeons may favor PKP over DALK for convenience. However, using a system that would significantly lower failure rates, may make DALK a more attractive option, albeit involving longer preparation and set up times.

4.2.3 Insertion angle

The data suggests that successful bubble formation occurred more likely following a shallow insertion angle, while unsuccessful trials more likely followed a steep insertion angle (see *Illustration 9*). Mean tunnel length however was similar in successful and failed cases. To investigate this further, a separate sample of 11 porcine eyes was cannulated. 5 out of 6 cases with entry angle set to 23.5 degrees were successful. All 5 trials with cannula entry angle set

to 30 degrees led to superficial air deposits and failure (Jablonka et al., 2020) (see *Illustration 11*).

The above-mentioned data allows to assume that shallower entry angles (~23 degrees) increase the chance, and steeper entry angles (~30 degrees) decrease the chance of successful deep air deposit. To our knowledge, this has not yet been further investigated and remains a potential topic of interest for future research.

4.2.4 Mean tunnel length

Mean tunnel length has not shown significant difference in robot-assisted and manual trials and as mentioned above, was quite similar in successful and unsuccessful trials. The data does not suggest any trend regarding success or failure, which may also be due to the small sample size of unsuccessful trials. Further research may be considered, as to our knowledge, tunnel length has not yet been investigated regarding surgery outcome. Naturally, tunnel length must be sufficient as to reach a sufficient depth and also, ensure that no air leakage occurs (Singh et al., 2021).

4.2.5 Mean duration of surgery

Duration of robot-assisted trials exceeded the duration of manual trials by 49 seconds on average. Since procedure time did not include robot preparation and calibration, it is fair to assume an even longer duration in robot-assisted procedures. Potentially, this is because the robot is maneuvered indirectly by utilizing the 3D-mouse. Since the latter is a mapped representation of the actual intended movement, it may not be assumed as naturally as maneuvering the syringe by hand. It is therefore conceivable that more concentration and practice may be required, which may in turn explain a longer surgery duration.

If applicable in clinical procedures, robotic assistance may in total require longer surgery time. However, this may be negligible depending on whether it contributes to a successful outcome.

4.3 Limiting factors

4.3.1 Setting

The experiments were performed on porcine instead of human corneas. This may be an adequate simulation material for some experiments; however, it is questionable whether that is the case for DALK simulations.

As previously mentioned in 4.2.2, porcine corneas were shown to have stronger adhesions between layers (Zeng et al., 2001; Guo et al., 2020), which is due to the young age (~6 months) at which they are usually slaughtered. Porcine corneas are typically thicker than human corneas (Zeng et al., 2001; Martola et al., 1968), with studies reporting averages around 670 microns in in vivo porcine corneas (Faber et al., 2014) and 1000 microns in ex-vivo porcine corneas (Jay et al., 2008). The human cornea in turn comprises 550 microns in thickness (Martola et al., 1968). They are also reported to be more elastic (Zeng et al., 2001). Ideally, human corneas should be considered for further experiments, as has been done in the study conducted by Draelos et al. (2020). However, it is important to note that use of porcine material enables large sample sizes without waste of potential human donor corneas. It is the reason why porcine corneas were used in this study.

The rubber base used to fix the porcine eyes made them easily accessible. The actual human orbit encapsules the eye, and facial structures such as the brow area and the nose make it oftentimes challenging to reach the desired structures. Robot placement would still need to be tested on human head models to see if the mounted instruments could reach the desired eye structures. Another thing to be considered is that during a clinical operation, body movement of the narcotized patient may occur, for example due to breathing. Movement of the tissue is not accounted for in the robotic setup. Apart from the above-mentioned, rather specific limiting factors, further sources of error include inaccuracies in robot- or OCT-calibration.

Further limiting factors address intraoperative OCT. In our experiments, it is necessary to continuously adjust the acquired cross section of the cannula to ensure depth information at any point in time throughout the procedure. This may require the surgeon to be more concentrated, which may in turn lead to a higher failure rate.

Most importantly, OCT cannula segmentation and thus, its accurate spatial resolution and localization within the cornea, can be approximated, but not accurately represented (Zhou et al., 2017). Difficulties include image speckle, low contrast, signal loss due to shadowing, and refraction artifacts (Rieke et al., 2015). More importantly, however, the cannula in OCT images and has illusory needle reflection (Adebar et al., 2014). As for postoperative analysis, the deviations were more easily controlled for. However, during insertion, the surgeon had to assume the instrument's true localization below the shadow in the real-time projections, which may have contributed to more conservative insertion. Certainly, it made the system less intuitive and thus not adequate for clinical application.

Accurate visualization of ophthalmic surgery instruments in OCT is challenging but has promising implications. It remains a topic of interest for further research.

4.3.2 Validity

In our studies, trials post air-injection have been considered successful when deep air deposit was visible with a demarcation plane located right above the DM. However, no actual pneumo-dissection occurred, due to the composition of the porcine corneas (see 4.3.1). It is thus questionable whether the named events were valid indicators of a potentially successful big-bubble formation. On the other hand, studies using human corneas could display an actual dissection of the DM and corneal stroma in OCT acquisitions (De Benito-Llopis, 2014).

Additionally, micro-perforation may be present, but not be visible in OCT. Failure due to micro-perforation was thus not respected in this study.

Regarding angle analysis, it is important to note that test captures in manual trials may not be valid, as they may deviate during the actual insertion. The second set of samples was therefore analysed by pre-setting the angle using the robot. Other than in manual performance, by aid of the robot, the priorly determined angle could be maintained throughout insertion and thus present a valid measure.

4.3.3 Feasibility

As discussed in 4.2, it is conceivable that novice surgeons may benefit from getting accustomed to the procedure aided by intraoperative OCT or a coupled system including robotic assistance. However, if novice surgeons start to rely on these support tools, they may not be able to perform DALK manually. This is in turn may be a downside, since many operation rooms are not equipped with intraoperative OCT, and purchasing a robot may not be affordable for some medical institutions. Utilization of the coupled system should thus be limited to the introduction to the technique.

In turn, surgeons who are experienced with DALK procedure may find it hard to get used to the robotic system, which requires its remote controlling as well. Experienced surgeons may not want to abort their usual technique and may also not see any benefit in using it. If they choose to adopt the system, the familiarization with the system may take a lot of training time. If employed on the patient, complication rate may initially rise, as the surgeons may have trouble applying the system at first and replacing their usual technique.

Employing a robot in the operation room furthermore raises questions on how to perform its placement, calibration, and the handling of its remote control in a way that it does not compromise on sterility. It is necessary to conduct further experiments that include solutions for sterile conditions as well.

5. CONCLUSIONS

It could be demonstrated in this study that inexperienced surgeons were able to perform DALK cannula insertion with subsequent air injection using both, manual and robot-assisted technique, along with intraoperative OCT monitoring throughout the procedure. Both manual and robot-assisted settings showed success rates consistent with similar studies as well as clinical statistics of DALK success rates. We believe that tremor management and real-time depth information account for higher accuracy in movements and thus account for these findings.

Using the robot, a depth of a mean of 84% could be achieved among successful trials. This was significantly deeper than in manual setting. It is also consistent with findings by recent studies comparing a cooperative system of OCT-imaging and robotic aid against manual surgery without imaging.

Since a depth surpassing 79% increases likelihood of successful big-bubble formation, it is feasible that reaching this depth without compromising on success rate may be beneficial. It may increase the probability of successful big bubble formation by reaching higher depths safely, thus lessen the numbers of conversion to PKP.

However, it is necessary to conduct further experimental research on robotic aid in DALK. It should be simulated on human corneas such as in the setting of the work by Draelos et al. (2020). Human corneal stroma is thinner and DM and stroma display actual pneumo-dissection in OCT after air injection.

The employment of the surgical robot should furthermore be tested in a more realistic setting, involving embedding eyes in human head and orbit models.

With DALK involving many benefits for the patient, for instance longer graft durability due to significantly less graft rejection, it is conceivable that working towards making the

procedure easier to learn and perform is worthwhile. Involving robotic aid and real-time OCT imaging may present a first step towards improving DALK success rates.

6. REFERENCES

Abdelkader, A., & Kaufman, H. E. (2011). Descemetic versus pre-descemetic lamellar keratoplasty: Clinical and confocal study. *Cornea, 30*(11), 1244–1252. DOI: 10.1097/ICO.0b013e318219bc1a

Adamis, A. P., Filatov, V., Tripathi, B. J., & Tripathi, R. C. (1993). Fuchs' endothelial dystrophy of the cornea. *Survey of Ophthalmology, 38*(2), 149–168.

Adebar, T. K., Fletcher, A. E., & Okamura, A. M. (2014). 3-D ultrasound-guided robotic needle steering in biological tissue. *IEEE Transactions on Biomedical Engineering, 61*(10), 2899–2910. DOI: 10.1109/TBME.2014.2334309

Alio, J. L., Abdelghany, A. A., Barraquer, R., Hammouda, L. M., & Sabry, A. M. (2015). Femtosecond laser assisted deep anterior lamellar keratoplasty outcomes and healing patterns compared to manual technique. *BioMed Research International, 2015*, 397891. DOI: 10.1155/2015/397891

Al-Mujaini, A., Al-Kharusi, N., Thakral, A., & Wali, U. K. (2009). Bacterial keratitis: Perspective on epidemiology, clinico-pathogenesis, diagnosis and treatment. *Sultan Qaboos University Medical Journal, 9*(2), 184–195. DOI: 10.18295/2075-0528.2789

Ang, M., Mehta, J. S., Arundhati, A., & Tan, D. T. H. (2009). Anterior lamellar keratoplasty over penetrating keratoplasty for optical, therapeutic, and tectonic indications: A case series. *American Journal of Ophthalmology, 147*(4), 697–702.e2. DOI: 10.1016/j.ajo.2008.10.002

Anwar, M., & Teichmann, K. D. (2002). Big-bubble technique to bare Descemet's membrane in anterior lamellar keratoplasty. *Journal of Cataract & Refractive Surgery, 28*(3), 398–403. DOI: 10.1016/s0886-3350(01)01181-6

Archila, E. A. (1984). Deep lamellar keratoplasty dissection of host tissue with intrastromal air injection. *Cornea, 3*(3), 217–218.

Ardjomand, N., Hau, S., McAlister, J. C., Bunce, C., Galaretta, D., Tuft, S. J., & Larkin, D. F. (2007). Quality of vision and graft thickness in deep anterior lamellar and penetrating corneal allografts. *American Journal of Ophthalmology, 143*(2), 228–235. DOI: 10.1016/j.ajo.2006.10.043

Au, J., Goshe, J., Dupps, W. J., Srivastava, S. K., & Ehlers, J. P. (2015). Intraoperative optical coherence tomography for enhanced depth visualization in deep anterior lamellar keratoplasty from the PIONEER study. *Cornea, 34*(9), 1039–1043. DOI: 10.1097/ICO.0000000000000508

Barr, J. T., Wilson, B. S., Gordon, M. O., Rah, M. J., Riley, C., Kollbaum, P. S., & Zadnik, K. (2006). Estimation of the incidence and factors predictive of corneal scarring in the Collaborative Longitudinal Evaluation of Keratoconus (CLEK) study. *Cornea, 25*(1), 16–25. DOI: 10.1097/01.ico.0000164831.87593.08

Barraquer, J. I. (1950). Technique of Penetrating Keratoplasty. *American Journal of Ophthalmology, 33*, 6–17. DOI: 10.1016/0002-9394(50)91080-4

Barrientez, B., Nicholas, S. E., Whelchel, A., Sharif, R., Hjortdal, J., & Karamichos, D. (2019). Corneal injury: Clinical and molecular aspects. Experimental Eye Research, 186, 107709. DOI: 10.1016/j.exer.2019.107709

Cao, Y., Zhang, W., Wu, J., Zhang, H., & Zhou, H. (2017). Peripheral ulcerative keratitis associated with autoimmune disease: Pathogenesis and treatment. Journal of Ophthalmology, 2017, 7298026. DOI: 10.1155/2017/7298026

Castillejo Becerra, C. M., Bourne, W. M., & Patel, S. V. (2023). Bilateral simultaneous penetrating keratoplasty: A 40-year odyssey. *Cornea Open, 2*, e0011. DOI: 10.1097/coa.0000000000000011

Dapena, I., Ham, L., & Melles, G. R. (2009). Endothelial keratoplasty: DSEK/DSAEK or DMEK - the thinner the better? *Current Opinion in Ophthalmology, 20*(4), 299–307. DOI: 10.1097/ICU.0b013e32832b8d18

Dartt, D. A., & Willcox, M. D. P. (2013). Complexity of the tear film: Importance in homeostasis and dysfunction during disease. *Experimental Eye Research, 117*, 1–3. DOI: 10.1016/j.exer.2013.10.008

De Benito-Llopis, L., Mehta, J. S., Angunawela, R. I., Ang, M., & Tan, D. T. H. (2014). Intraoperative anterior segment optical coherence tomography: A novel assessment tool during deep anterior lamellar keratoplasty. *American Journal of Ophthalmology, 157*(2), 334–341.e3. DOI: 10.1016/j.ajo.2013.10.001

DelMonte, D. W., & Kim, T. (2011). Anatomy and physiology of the cornea. *Journal of Cataract & Refractive Surgery, 37*(3), 588–598. DOI: 10.1016/j.jcrs.2010.12.037

Draelos, M., Tang, G., Keller, B., Kuo, A., Hauser, K., & Izatt, J. (2020). Optical coherence tomography guided robotic needle insertion for deep anterior lamellar keratoplasty. *IEEE Transactions on Biomedical Engineering, 67*(8), 2073–2083. DOI: 10.1109/TBME.2019.2954505

Draelos, M., Keller, B., Tang, G., Kuo, A., Hauser, K., & Izatt, J. (2018). Real-time image-guided cooperative robotic assist device for deep anterior lamellar keratoplasty. In *2018 IEEE International Conference on Robotics and Automation (ICRA)* (pp. 4013–4018). DOI: 10.1109/ICRA.2018.8463153

Dua, H. S., Faraj, L. A., Said, D. G., Gray, T., & Lowe, J. (2013). Human corneal anatomy redefined: A novel pre-Descemet's layer (Dua's layer). *Ophthalmology, 120*(9), 1778–1785. DOI: 10.1016/j.ophtha.2013.12.021

El-Massry, A., Ibrahim, O., Abdalla, M., Osman, I., & Mahmoud, S. (2021). Safety and indicative effectiveness of porcine corneal lenticular implants in patients with advanced keratoconus and post LASIK ectasia: A retrospective clinical study. *Clinical Ophthalmology, 15*, 3165–3171. DOI: 10.2147/OPTH.S325666

Espandar, L., & Carlson, A. N. (2013). Lamellar keratoplasty: A literature review. *Journal of Ophthalmology, 2013*, Article ID 184570. DOI: 10.1155/2013/894319

Faber, C., Scherfig, E., Prause, J. U., & Sørensen, K. E. (2014). Corneal thickness in pigs measured by ultrasound pachymetry in vivo. *Scandinavian Journal of Laboratory Animal Science, 35*, 39–43. DOI: 10.23675/sjlas.v35i1.139

Farid, M., & Steinert, R. F. (2009). Deep anterior lamellar keratoplasty performed with the femtosecond laser zigzag incision for the treatment of stromal corneal pathology and ectatic disease. *Journal of Cataract & Refractive Surgery, 35*(5), 809–813. DOI: 10.1016/j.jcrs.2009.01.012

Fasolo, A., Galzignato, A., Pedrotti, E., Chierego, C., Cozzini, T., Bonacci, E., & Marchini, G. (2021). Femtosecond laser-assisted implantation of corneal stroma lenticule for keratoconus. *International Ophthalmology, 41*(6), 1949–1957. DOI: 10.1007/s10792-021-01739-8

Fogla, R. (2013). Deep anterior lamellar keratoplasty in the management of keratoconus. *Indian Journal of Ophthalmology, 61*(9), 465. DOI: 10.4103/0301-4738.116061

Fournié, P., Malecaze, F., Coullet, J., & Arné, J.-L. (2007).
Variant of the big bubble technique in deep anterior lamellar keratoplasty. *Journal of Cataract & Refractive Surgery, 33*(3), 371–375. DOI: 10.1016/j.jcrs.2006.10.053

Gabriele, M. L., Wollstein, G., Ishikawa, H., Kagemann, L., Xu, J., Folio, L. S., & Schuman, J. S. (2011).
Optical coherence tomography: History, current status, and laboratory work. *Investigative Ophthalmology & Visual Science, 52*(5), 2425–2436. DOI: 10.1167/iovs.10-6312

Gajecka, M., & Nowak, D. (2011). The genetics of keratoconus. *Middle East African Journal of Ophthalmology, 18*(1), 2–6. DOI: 10.4103/0974-9233.75876

Gorovoy, M. S. (2006). Descemet-stripping automated endothelial keratoplasty. *Cornea, 25*(8), 886–889. DOI: 10.1097/01.ico.0000214224.90743.01

Goweida, M. B., Abuelkheir, A., El-Menawy, W., & Mahmoud, S. (2020**).** Dynamics of big bubble formation during deep anterior lamellar keratoplasty in eyes with advanced keratoconus. *Clinical Ophthalmology, 14*, 4305–4310. DOI: 10.2147/OPTH.S277738

Guilbert, E., Bullet, J., Sandali, O., Basli, E., Laroche, L., & Borderie, V. M. (2013). Long-term rejection incidence and reversibility after penetrating and lamellar keratoplasty. *American Journal of Ophthalmology, 155*(3), 560–569.e2. DOI: 10.1016/j.ajo.2012.09.027

Guo, S., Sarfaraz, N. R., Gensheimer, W. G., Krieger, A., & Kang, J. U. (2020). Demonstration of optical coherence tomography guided big bubble technique for deep anterior lamellar keratoplasty (DALK). *Sensors, 20*(2), 428. DOI: 10.3390/s20020428

Güell, J. L., El Husseiny, M. A., Manero, F., Gris, O., & Elies, D. (2014). Historical review and update of surgical treatment for corneal endothelial diseases. *Ophthalmology and Therapy, 3*(1), 1–15. DOI: 10.1007/s40123-014-0022-y

Hallermann, W. (1959). Some remarks on keratoplasty. *Klinische Monatsblätter für Augenheilkunde, 135*, 252–259.

Ham, L., Dapena, I., Van Luijk, C., Van der Wees, J., & Melles, G. R. J. (2009). Descemet membrane endothelial keratoplasty (DMEK) for Fuchs endothelial dystrophy: Review of the first 50 consecutive cases. *Eye, 23*(10), 1990–1998. DOI: 10.1038/eye.2008.393

Huang, O. S., Htoon, H. M., Chan, A. M., Tan, D., & Mehta, J. S. (2019). Incidence and outcomes of intraoperative Descemet membrane perforations during deep anterior lamellar keratoplasty. *American Journal of Ophthalmology, 199*, 9–18. DOI: 10.1186/s13054-020-03112-0

Izadi, M., Jonaidi-Jafari, N., Pourazizi, M., Alemzadeh-Ansari, M. H., & Hoseinpourfard, M. J. (2018). Photokeratitis induced by ultraviolet radiation in travelers: A major health problem. *Journal of Postgraduate Medicine, 64*(1), 40–46. DOI: 10.4103/jpgm.JPGM_52_17

Jablonka, A.-M., Maierhofer, N. A., Roodaki, H., Eslami, A., Zapp, D., Nasseri, A., & Lohmann, C. P. (2020). The effect of needle entry angle on bubble formation in DALK using the big-bubble technique. *Investigative Ophthalmology & Visual Science, 61*(7), 1862

Jay, L., Brocas, A., Singh, K., Kieffer, J.-C., Brunette, I., & Ozaki, T. (2008). Determination of porcine corneal layers with high spatial resolution by simultaneous second and third harmonic generation microscopy. *Optics Express, 16*(21), 16284–16293. DOI: 10.1364/OE.16.016284

Jain, S., Azar, D. T., & Pineda, R. (2002). Management of astigmatism after corneal trauma. *International Ophthalmology Clinics, 42*(3), 47–55. DOI: 10.1097/00004397-200207000-00007

Jhanji, V., Sharma, N., & Vajpayee, R. B. (2010). Intraoperative perforation of Descemet's membrane during "big bubble" deep anterior lamellar keratoplasty. *International Ophthalmology, 30*(3), 291–295. DOI: 10.1007/s10792-009-9334-7

Karimian, F., & Feizi, S. (2010). Deep anterior lamellar keratoplasty: Indications, surgical techniques and complications. *Middle East African Journal of Ophthalmology, 17*(1), 28–37. DOI: 10.4103/0974-9233.61214

Khaja, W. A., Grover, S., Kelmenson, A. T., Ferguson, L. R., Sambhav, K., & Chalam, K. V. (2015). Comparison of central corneal thickness: Ultrasound pachymetry versus slit-lamp optical coherence tomography, specular microscopy, and Orbscan. *Clinical Ophthalmology, 9*, 1065–1070. DOI: 10.2147/OPTH.S81376

Kivelä, T., Tarkkanen, A., McLean, I., Ghiso, J., Frangione, B., & Haltia, M. (1993). Immunohistochemical analysis of lattice corneal dystrophies types I and II. *British Journal of Ophthalmology, 77*(12), 799–804. DOI: 10.1136/bjo.77.12.799

Kocaba, V., Damour, O., Auxenfans, C., & Burillon, C. (2018). Descemet's membrane endothelial keratoplasty: Indication, technique chirurgicale, gestion postopératoire et revue de la littérature. *Journal Français d'Ophtalmologie, 41*(4), 368–381. DOI: 10.1016/j.jfo.2017.12.005

Koçluk, Y., Alyamaç Sukgen, E., & Burcu, A. (2017). Comparison of outcomes in patients who underwent deep anterior lamellar keratoplasty and those converted to penetrating keratoplasty. *Türk Oftalmoloji Dergisi, 47*(2), 63–67. DOI: 10.4274/tjo.25675

Kodavoor, S., Rathi, N., & Dandapani, R. (2022). Complications in deep anterior lamellar keratoplasty – A retrospective interventional analysis in a large series. *Indian Journal of Ophthalmology, 70*(11), 3501–3506. DOI: 10.4274/tjo.25675

Krstić, R. V. (1985). Transplantation, implantation, and explantation. In *General histology of the mammal* (pp. 12–13). Springer Berlin Heidelberg.

Le, R., Yucel, N., Khattak, S., Yucel, Y. H., Prud'homme, G. J., & Gupta, N. (2017). Current indications and surgical approaches to corneal transplants at the University of Toronto: A clinical-pathological study. *Canadian Journal of Ophthalmology, 52*(1), 74–79. DOI: 10.1016/j.jcjo.2016.07.005

Leccisotti, A. (2007). Descemet's membrane perforation during deep anterior lamellar keratoplasty: Prognosis. *Journal of Cataract and Refractive Surgery, 33*(5), 825–829. DOI: 10.1016/j.jcrs.2007.02.016

Lee, R. M., Lam, F. C., Georgiou, T., Paul, B., Then, K. Y., Mavrikakis, I., Avadhanam, V. S., & Liu, C. S. C. (2012). Suturing techniques and postoperative management in penetrating keratoplasty in the United Kingdom. *Clinical Ophthalmology, 6*, 1335–1340. DOI: 10.2147/OPTH.S35460

Lin, Z.-N., Chen, J., & Cui, H.-P. (2016). Characteristics of corneal dystrophies: A review from clinical, histological and genetic perspectives. *International Journal of Ophthalmology, 9*(7), 904–913. DOI: 10.18240/ijo.2016.06.20

Liu, H., Chen, Y., Wang, P., Li, B., Wang, W., Su, Y., & Sheng, M. (2015). Efficacy and safety of deep anterior lamellar keratoplasty vs. penetrating keratoplasty for keratoconus: A meta-analysis. *PLoS ONE, 10*(1), e0113332. DOI: 10.1371/journal.pone.0113332

Lorenzetti, D. W., Uotila, M. H., Parikh, N., & Kaufman, H. E. (1967). Central cornea guttata. Incidence in the general population. *American Journal of Ophthalmology, 64*(6), 1155–1158.

Luengo-Gimeno, F., Tan, D. T., & Mehta, J. S. (2011). Evolution of Deep Anterior Lamellar Keratoplasty (DALK). *The Ocular Surface, 9*(2), 98–110. DOI: 10.1016/s1542-0124(11)70017-9

Maier, M. M., Nasseri, A., Framme, C., Bohnacker, S., Becker, M. D., Heinrich, D., Agostini, H., Feucht, N., Lohmann, C. P., & Hattenbach, L. O. (2018). Die intraoperative optische Kohärenztomografie in der Netzhaut-Glaskörper-Chirurgie: Aktuelle Erfahrungen und Ausblick auf künftige Entwicklungsschritte. *Klinische Monatsblätter für Augenheilkunde, 235*(9), 1028–1034. DOI: 10.1055/s-0043-106304

Malyugin, B. E., Belodedova, A., Antonova, O., Gelyastanov, A., Tuuminen, R., Levinger, E., Achiron, A., & Knyazer, B. (2023). Clinical comparison of manual and laser-cut corneal tunnel for intrastromal air injection in femtosecond laser-assisted deep anterior lamellar keratoplasty (DALK). *Graefe's Archive for Clinical and Experimental Ophthalmology, 261*(1), 185–191. DOI: 10.1007/s00417-022-05765-9

Mannis, M. J., & Krachmer, J. H. (1981). Keratoplasty: A historical perspective. *Survey of Ophthalmology, 25*(4), 333–338. DOI: 10.1016/0039-6257(81)90159-4

Martola, E.-L. (1968). Central and peripheral corneal thickness: A clinical study. *Archives of Ophthalmology, 79*(1), 28. DOI: 10.1001/archopht.1968.03850040030009

McGhee, C., Crawford, A., & Patel, D. (2013). A brief history of corneal transplantation: From ancient to modern. *Oman Journal of Ophthalmology, 6*(1), 12–14. DOI: 10.4103/0974-620X.122289

Melles, G. R., Lander, F., Rietveld, F. J., Remeijer, L., Beekhuis, W. H., & Binder, P. S. (1999). A new surgical technique for deep stromal, anterior lamellar keratoplasty. *British Journal of Ophthalmology, 83*(3), 327–333. DOI: 10.1136/bjo.83.3.327

Melles, G. R., Ong, T. S., Ververs, B., & van der Wees, J. (2006). Descemet membrane endothelial keratoplasty (DMEK). *Cornea, 25*(9), 987–990. DOI: 10.1097/01.ico.0000248385.16896.34

Merali, F. I. (2014). Calcific Band Keratopathy. In U. Schmidt-Erfurth & T. Kohnen (Eds.), *Encyclopedia of Ophthalmology* (pp. 1–2). Springer Berlin Heidelberg.

Modabber, M., & Mannis, M. (2023). Penetrating Keratoplasty in Keratoconus. In *Keratoconus* (pp. 479–486). Elsevier. DOI: 10.1016/B978-0-323-75978-6.00032-7.

Moffatt, S. L., Cartwright, V. A., & Stumpf, T. H. (2005). Centennial review of corneal transplantation. *Clinical and Experimental Ophthalmology, 33*(6), 642–657.

Myerscough, J., Bovone, C., Mimouni, M., Elkadim, M., Rimondi, E., & Busin, M. (2019). Factors predictive of double anterior chamber formation following deep anterior lamellar keratoplasty. *American Journal of Ophthalmology, 205*, 11–16. DOI: 10.1016/j.ajo.2019.03.026

Nakamura, T., Nishida, K., Dota, A., Adachi, A., Yamamoto, S., Maeda, N., Okada, M., & Kinoshita, S. (2000). Gelatino-lattice corneal dystrophy: Clinical features and mutational analysis. *American Journal of Ophthalmology, 129*(5), 665–666. DOI: 10.1016/s0002-9394(00)00369-x

Nanavaty, M. A., Vijjan, K. S., & Yvon, C. (2018). Deep anterior lamellar keratoplasty: A surgeon's guide. *Journal of Current Ophthalmology, 30*(4), 297–310. DOI: 10.1016/j.joco.2018.06.004

Ng, J. D., Nekola, M., Parmley, V. C., Richardson, M., & Mader, T. (1995**).** Comparison of three corneal trephines for use in therapeutic penetrating keratoplasties for large corneal perforations. *Ophthalmic Surgery, 26*(3), 209–215.

Nonpassopon, M., Niparugs, M., & Cortina, M. S. (2020). Boston Type 1 Keratoprosthesis: Updated perspectives. *Clinical Ophthalmology, 14*, 1189–1200. DOI: 10.2147/OPTH.S219270

Nuzzi, R., Trossarello, M., Bartoncini, S., Marolo, P., Franco, P., Mantovani, C., & Ricardi, U. (2020). Ocular complications after radiation therapy: An observational study. *Clinical Ophthalmology, 14*, 3153–3166. DOI: 10.2147/OPTH.S263291

Ozmen, M. C., Yesilirmak, N., Aydin, B., Ceylanoglu, K. S., Atalay, H. T., & Akata, F. (2018). Prediction of Descemet membrane perforation during deep anterior lamellar keratoplasty in patients with keratoconus with stromal scar. *Eye & Contact Lens, 44*(Suppl 2), S176–S179. DOI: 10.1097/ICL.0000000000000434

Pahor, D., Gracner, B., Falez, M., & Gracner, T. (2007**).** Changing indications for penetrating keratoplasty over a 20-year period, 1985–2004. *Klinische Monatsblätter für Augenheilkunde, 224*(2), 110–114. DOI: 10.1055/s-2007-962962

Pasricha, N. D., Shieh, C., Carrasco-Zevallos, O. M., Keller, B., Cunefare, D., Mehta, J. S., Farsiu, S., Izatt, J. A., Toth, C. A., & Kuo, A. N. (2016). Needle depth and big-bubble success in deep anterior lamellar keratoplasty: An ex vivo microscope-integrated OCT study. *Cornea, 35*(12), 1471–1477. DOI: 10.1097/ICO.0000000000000948

Patel, S., & Tutchenko, L. (2019). The refractive index of the human cornea: A review. *Contact Lens and Anterior Eye, 42*(6), 575–580. DOI: 10.1016/j.clae.2019.04.018

Rama, P., Knutsson, K. A., Razzoli, G., Matuska, S., Viganò, M., & Paganoni, G. (2013). Deep anterior lamellar keratoplasty using an original manual technique. *British Journal of Ophthalmology, 97*(1), 23–27. DOI: 10.1136/bjophthalmol-2011-301168

Reddy, J. C., Murthy, S. I., Vaddavalli, P. K., Garg, P., Ramappa, M., Chaurasia, S., Rathi, V., & Sangwan, V. S. (2015). Clinical outcomes and risk factors for graft failure after deep anterior lamellar keratoplasty and penetrating keratoplasty for macular corneal dystrophy. *Cornea, 34*(2), 171–176. DOI: 10.1097/ICO.0000000000000327

Reinhart, W. J., Musch, D. C., Jacobs, D. S., Lee, W. B., Kaufman, S. C., & Shtein, R. M. (2011). Deep anterior lamellar keratoplasty as an alternative to penetrating keratoplasty. *Ophthalmology, 118*(1), 209–218. DOI: 10.1016/j.ophtha.2010.11.002

Rieke, N., Tan, D. J., Alsheakhali, M., Federico Tombari, F., Belagiannis, V., & Navab, N. (2015). Surgical tool tracking and pose estimation in retinal microsurgery. In N. Navab, J. Hornegger, W. M. Wells, & A. Frangi (Eds.), *Medical Image Computing and Computer-Assisted Intervention – MICCAI 2015* (Vol. 9349, pp. 266–273). Springer International Publishing.

Rosenberg, J. B., & Eisen, L. A. (2008). Eye care in the intensive care unit: Narrative review and meta-analysis. *Critical Care Medicine, 36*(11), 3151–3155. DOI: 10.1097/CCM.0b013e31818f0ee7

Santorum, P., Yu, A. C., Bertelli, E., & Busin, M. (2022). Microscope-integrated intraoperative optical coherence tomography–guided big-bubble deep anterior lamellar keratoplasty. *Cornea, 41*(1), 125–129. DOI: 10.1097/ICO.0000000000002826

Sari, E. S., Kubaloglu, A., Ünal, M., Llorens, D. P., Koytak, A., Ofluoglu, A. N., & Özertürk, Y. (2012). Penetrating keratoplasty versus deep anterior lamellar keratoplasty: Comparison of optical and visual quality outcomes. *British Journal of Ophthalmology, 96*(8), 1063–1067. DOI: 10.1016/j.ajo.2013.03.007

Schaub, F., Enders, P., Adler, W., Bachmann, B. O., Cursiefen, C., & Heindl, L. M. (2017). Impact of donor graft quality on deep anterior lamellar keratoplasty (DALK). *BMC Ophthalmology, 17*, 204. DOI: 10.1186/s12886-017-0600-6

Singh, B., Sharma, S., Bharti, N., & Bharti, S. (2021). A novel method of tunnel creation using intraoperative optical coherence tomography-guided deep anterior lamellar keratoplasty. *Indian Journal of Ophthalmology, 69*(12), 3743. DOI: 10.4103/ijo.IJO_531_21

Singh, P., Tyagi, M., Kumar, Y., Gupta, K., & Sharma, P. (2013). Ocular chemical injuries and their management. *Oman Journal of Ophthalmology, 6*(2), 83. DOI: 10.4103/0974-620X.116624

Sridhar, M. (2018). Anatomy of cornea and ocular surface. *Indian Journal of Ophthalmology, 66*(2), 190. DOI: 10.4103/ijo.IJO_646_17

Sridhar, M. (2004). Pellucid marginal corneal degeneration. *Ophthalmology, 111*(6), 1102–1107. DOI: 10.1016/j.ophtha.2003.09.035

Steven, P., Le Blanc, C., Lankenau, E., Krug, M., Oelckers, S., Heindl, L. M., Gehlsen, U., Huettmann, G., & Cursiefen, C. (2014). Optimising deep anterior lamellar keratoplasty (DALK) using intraoperative online optical coherence tomography (iOCT). *British Journal of Ophthalmology, 98*(7), 900–904. DOI: 10.1136/bjophthalmol-2013-304585

Stewart, O. G., & Morrell, A. J. (2003). Management of band keratopathy with excimer phototherapeutic keratectomy: Visual, refractive, and symptomatic outcome. *Eye, 17*(2), 233–237. DOI: 10.1038/sj.eye.6700327

Stübiger, N., Pleyer, U., Erb, C., & Thiel, H. J. (1995). Keratoplasty à chaud. *Ophthalmologe*, *92*(5), 427–432.

Sugita, J., & Kondo, J. (1997). Deep lamellar keratoplasty with complete removal of pathological stroma for vision improvement. *British Journal of Ophthalmology, 81*(3), 184–188. DOI: 10.1136/bjo.81.3.184

Tan, D. T., & Anshu, A. (2009). Anterior lamellar keratoplasty: 'Back to the future' – a review. *Clinical and Experimental Ophthalmology*. DOI: 10.1111/j.1442-9071.2009.02180.x

Tan, D. T. H., Anshu, A., Parthasarathy, A., & Htoon, H. M. (2010). Visual acuity outcomes after deep anterior lamellar keratoplasty: A case-control study. *British Journal of Ophthalmology, 94*(10), 1295–1299. DOI: 10.1136/bjo.2009.167528

Watson, S. L., Ramsay, A., Dart, J. K. G., Bunce, C., & Craig, E. (2004). Comparison of deep lamellar keratoplasty and penetrating keratoplasty in patients with keratoconus. *Ophthalmology, 111*(9), 1676–1682. DOI: 10.1016/j.ophtha.2004.02.010

Watson, S. L., Tuft, S. J., & Dart, J. K. G. (2006). Patterns of rejection after deep lamellar keratoplasty. *Ophthalmology, 113*(4), 556–560. DOI: 10.1016/j.ophtha.2006.01.006

Zeng, Y., Yang, J., Huang, K., Lee, Z., & Lee, X. (2001). A comparison of biomechanical properties between human and porcine cornea. *Journal of Biomechanics, 34*(5), 533–537. DOI: 10.1016/s0021-9290(00)00219-0

Zhao, Y., Jablonka, A.-M., Maierhofer, N. A., Roodaki, H., Eslami, A., Maier, M., Nasseri, M. A., & Zapp, D. (2023). Comparison of robot-assisted and manual cannula insertion in simulated big-bubble deep anterior lamellar keratoplasty. *Micromachines, 14*(6), 1261. DOI: 10.3390/mi14061261

Zhou, M., Roodaki, H., Eslami, A., Chen, G., Huang, K., Maier, M., Lohmann, C. P., Knoll, A., & Nasseri, M. A. (2017). Needle segmentation in volumetric optical coherence tomography images for ophthalmic microsurgery. *Applied Sciences, 7*(7), 748. DOI: 10.3390/app7080748